CEFET/RJ
DIRETORIA DE PESQUISA E PÓS-GRADUAÇÃO

INFLUÊNCIA DE TRATAMENTO MECÂNICO SUPERFICIAL EM VIDA DE FADIGA DE JUNTAS COLADAS SUBMETIDAS AO CISALHAMENTO

Svetlana Nikolaevna Magalhães Ferreira

Dissertação de Mestrado apresentada ao Programa de Pós-graduação em Engenharia Mecânica e Tecnologia de Materiais, Centro Federal de Educação Tecnológica Celso Suckow da Fonseca, CEFET/RJ, como parte dos requisitos à obtenção do título de mestre.

Orientadores:
Silvio Romero de Barros
Paulo Pedro Kenedi

Rio de Janeiro
fevereiro de 2016

INFLUÊNCIA DE TRATAMENTO MECÂNICO SUPERFICIAL EM VIDA DE FADIGA DE JUNTAS COLADAS SUBMETIDAS AO CISALHAMENTO.

Dissertação de Mestrado apresentada ao Programa de Pós-graduação em Engenharia Mecânica e Tecnologia de Materiais do Centro Federal de Educação Tecnológica Celso Suckow da Fonseca, CEFET/RJ, como parte dos requisitos à obtenção do título de mestre.

Svetlana Nikolaevna Magalhães Ferreira

Aprovada por:

_____

Prof. Doutor Silvio Romero de Barros

_____

Prof. Doutor Paulo Pedro Kenedi (coorientador)

_____

Prof. Doutor Ricardo Alexandre Amar de Aguiar

_____

Prof. Doutor Luiz Carlos da Silva Nunes - UFF

Rio de Janeiro
fevereiro de 2016

Ficha catalográfica elaborada pela Biblioteca Central do CEFET/RJ

F383 Ferreira, Svetlana Nikolaevna Magalhães
Influência de tratamento mecânico superficial em vida de fadiga de juntas coladas submetidas ao cisalhamento / Svetlana Nikolaevna Magalhães Ferreira.—2016.
xiii, 56f. + apêndice : il. (algumas color.) , grafs. , tabs. ; enc.

Dissertação (Mestrado) Centro Federal de Educação Tecnológica Celso Suckow da Fonseca , 2016.
Bibliografia : f. 54-56
Orientadores : Silvio Romero de Barros
Paulo Pedro Kenedi

1. Engenharia mecânica. 2. Juntas (Engenharia) – Fadiga. 3. Cisalhamento. I. Barros, Silvio Romero de (Orient.). II. Kenedi, Paulo Pedro (Orient.). III. Título.

CDD 620.1126

Agradecimentos.

Ao Centro Federal de Educação Tecnológica Celso Suckow da Fonseca pela oportunidade de fazer o mestrado.

Agradeço aos meus orientadores o Dr. Silvio Romero de Barros e Dr. Paulo Pedro Kenedi e professor Dr. Luis Felipe Guimaraes de Souza por fornecerem as ferramentas teóricas e experimentais e o apoio professional e emocional, que me mantiveram no caminho do aprendizado e da execução deste trabalho.

Ao meu marido Fábio Magalhães e minha mãe Nadezhda Mikhailovna pela paciência e apoio nos momentos mais difíceis.

Aos colegas Diego Santos de Moura, Hiron Akira, Armando José Moraes de Azevedo por troca de ideias, palavras de incentivo e aprendizado.

A todos os professores do Programa de Pós-graduação em Engenharia Mecânica e Materiais de Mestrado.

Às agências de fomento CNPq, CAPES e FAPERJ por suporte financeiro.

“A melhor forma de prever o futuro é criá-lo”

Peter Drucker

Resumo

INFLUÊNCIA DE TRATAMENTO MECÂNICO SUPERFICIAL EM VIDA DE FADIGA DE JUNTAS COLADAS SUBMETIDAS AO CISALHAMENTO

Svetlana Nikolaevna Magalhães Ferreira

Orientadores:

Sílvio Romero de Barros

Paulo Pedro Kenedi

Resumo da dissertação submetida ao Programa de Pós-graduação em Engenharia Mecânica e Tecnologia de Materiais do Centro Federal de Educação Tecnológica Celso Suckow da Fonseca – CEFET/RJ, como parte dos requisitos necessários à obtenção do título de mestre.

Componentes estruturais estão usualmente submetidas ao carregamento de fadiga. Longa vida de fadiga das juntas coladas é uma das vantagens principais quando se escolhe usá-la em lugar de juntas convencionais. Adicionalmente, colagem evita concentradores de tensões nas juntas e permite juntar materiais diferentes. Por outro lado, atualmente o mecanismo de falha nas juntas coladas não está explicado completamente, o que limita o uso da colagem nas indústrias.

O tratamento superficial mecânico de substratos influência diretamente a qualidade de juntas coladas. O objetivo do tratamento superficial é otimizar a interface da junta colada. Presente trabalho apresenta uma investigação da influência da rugosidade do substrato na vida de fadiga de juntas coladas. Para realização do trabalho, as juntas foram coladas com epóxi estrutural usando substratos de aço de baixo teor de carbono, com aplicação de três diferentes tratamentos mecânicos: jateamento com granalha, com areia, e abrasão com escova. As juntas foram testadas monotonamente e sob a carga alternada, no formato *end-notched flexure*, na condição de ambiente normal.

A influência do tratamento mecânico superficial para vida de fadiga de juntas coladas foi avaliada como significativa. Analise realizada no trabalho revelou os tratamentos de granalha e de areia como as melhores escolhas para tratamento mecânico superficial para substratos de juntas coladas.

Palavras-chaves:

Fadiga; Tratamento superficial; Juntas coladas.

Rio de Janeiro

fevereiro de 2016

Abstract

INFLUENCE OF SURFACE MECHANICAL TREATMENT ON FATIGUE LIFE OF BONDED JOINTS UNDER SHEAR STRENTH

Svetlana Nikolaevna Magalhães Ferreira

Advisors:

Silvio Romero de Barros

Paulo Pedro Kenedi

Abstract of dissertation submitted to Programa de Pós-graduação em Engenharia Mecânica e Tecnologia de Materiais do Centro Federal de Educação Tecnológica Celso Suckow da Fonseca, CEFET/RJ as partial fulfillment of the requirements for the degree of master.

Structural components are usually subjected to fatigue loadings. Longer fatigue life of adhesively bonded joints is one of the main advantages of using bonded joints instead of conventional joining techniques In addition adhesively bonded joints present fewer source of stress concentration and allow joining different materials. However, current incomplete understanding of adhesive bond failures still limits its broad using in industry.

Mechanical preparation of bonded surface influences directly in bonded joint quality. The purpose of the surface treatment is the adhesion improvement of joint interface. This work is carry out of investigation the influence of surface roughness of bonded joints on fatigue life. To do that, sand blasting, grit blasting, bristle blasting surface mechanical treatment were applied on the surface of mild steel substrates and the joints were bonded with structural epoxy. The joints were tested statically and under high cycle fatigue conditions in end-notched flexure format, at normal ambient conditions.

The influence of substrate mechanical treatment in fatigue life of bonded joints was evaluated as significant. Comparison analysis revealed that grit blasting and sand blasting are the best choice as a mechanical surface treatment for metallic adherents to be bonded.

Keywords:

Fatigue; Surface treatment; Bonded joints.

Rio de Janeiro

fevereiro 2016

Contents

I. Introduction 1
II. General aspects of structural bonding. 3
II.1. Adhesion theories 4
II.2. Surface tension or surface free energy 5
II.3. Roughness 9
II.4. Weak boundary layer 10
II.5. Surface treatment 13
II.6. Adhesives for metal bonding 14
II.7. Fatigue testing parameters for metal bonded joints 15
II.8. Minimum number of specimens for fatigue testing 15
II.9. Review of recent works 15
III. Experimental procedure 22
III.1. Materials and methods 22
III.2. Monotonic thick adherent shear testing 26
III.3. Monotonic end-notched flexure testing 28
III.4. Dynamic end-notched flexure testing. 29
IV. Results and discussions 32
IV.1. Substrate mechanical treatment and roughness parameters. 32
IV.2. Thick adherent shear testing in monotonic regime. 34
IV.3. Monotonic end-notched flexure testing. 36
IV.4. Dynamic end-notched flexure testing 37
IV.5. Failure locus analysis 39
IV.6. Load analysis 42
IV.7. Crack length analyses 44
IV.8. Crack propagation analyses 46
V. Conclusions and suggestions 52
V.1. Conclusions. 52
V.2. Suggestions for future works 52
Presentations of the work. 62
References. 54
Appendix. 57

List of figures

Figure II.1 Intermolecular forces. DA SILVA *et al*. (2007). 6
Figure II.2 The illustration of the equilibrium force balance according to Young's equation. Available in: < http://www.jpbsonline.org/article.asp?issn=0975-7406;year=2011;volume=3;issue=1;spage=89;epage=100;aulast=Shaikh> 6
Figure II.3 Liquid drop on solid surface. Available in: < https://www.teachengineering.org/view_lesson.php?url=collection/duk_/lessons/duk_surfacetensionunit_lessons/duk_surfacetensionunit_less3.xml> 7
Figure II.4 The illustration of cohesive and adhesive force actuation in adhesive layer. Available in: < http://www.adhesives.org/adhesives-sealants/science-of-adhesion/adhesion-cohesion> ... 8
Figure II.5 The Illustration of Wenzel wetting theory. 8
Figure II.6 Average surface roughness, Ra. 10
Figure II.7 The Illustration of weak boundary layer: 1 – adhesive, 2 – impurities, entrapped air, chemical reactions, 3– adherent. 11
Figure II.8 Types of failure interface. 12
Figure III.1 Servo-hydraulic machine Instron 100kN. Available in: < http://www.azom.com/equipment-details.aspx?EquipID=1183> 22
Figure III.2 Specimen installation in servo-hydraulic machine. 23
Figure III.7 Stereoscopic loupe Metrimpex. 24
Figure III.8 Bonded joint with painted lateral side. 25
Figure III.9 3D roughness tester Talyscan 150. Available in: < http://www.hoskin.qc.ca/uploadpdf/Instrumentation/Taylor%20Hobson/hoskin_TSCAN150_44ad086f7458b.pdf> 25
Figure III.10 Contact roughness tester Mitutoyo. Available in: < http://www.lighttoolsupply.com/catalog/Manufacturers/Mitutoyo/Mitutoyo-Surftest-SJ-210-Portable-Surface-Roughness-Tester > 26
Figure III.11 Specimen dimension and configuration for TAST. 26
Figure III.12 Position of the TAST specimen in testing dispositive. 28
Figure III.13 End-notched flexure joint dimension and configuration. 28
Figure III.14 Typical load-displacement graphic. 30
Figure III.15 Typical load-displacement graphic at the end of the test. 30
Figure III.16 Load-time graphic. 31
Figure III.17 Displacement-cycles graphic. 31
Figure IV.1 Surface profiles after mechanical treatment: 33
a) grit blasted surface profile; b) sand blasted surface profile; c) bristle blasted surface profile. 33

Figure IV.2 TAST results obtained for all the specimens. 34
Figure IV.3 Failure interface of the specimens after thick adherent shear testing: a) grit blasted specimen, b) sand blasted specimen, c) bristle blasted specimen. 35
Figure IV.4 Load-displacement curve for static test of sand blasting specimens: 37
a) SP1 Py = 6,000N; b) SP2 Py = 6,400N; c) SP3 Py = 6,500N. 37
Figure IV.5 Grit blasted specimen after the testing in monotonic regime. 37
Figure IV.6 Load-cycles curves obtained for three types of substrate mechanical treatment.... 39
Figure IV.7 Load-displacement curve at the final phase of the fatigue test of the specimen M7T1(B). 40
Figure IV.8 Failure interfaces of tested specimens: a) grit blasted failure interface, b) sand blasted failure interface, c) bristle blasted failure interface. 41
Figure IV.9 Top view of fragile failure line of the sand blasted specimen (A). 41
Figure IV.10 The Inclination of the fragile failure line (lateral view). 42
Figure IV.11 Load-displacement curve at the final phase of the fatigue test of the sand blasted specimen tested under 50% of load level. 43
Figure IV.12 Load-displacement curve at the final phase of the fatigue test of the sand blasted specimen tested under 60% of load level. 43
Figure IV.13 Load-displacement curve at the final phase of the fatigue test of the sand blasted specimen tested under 70% of load level. 44
Figure IV.14 Load-displacement curve at the final phase of the fatigue test of the sand blasted specimen tested under 80% of load level. 44
Figure IV.15 Crack length diagram. 46
Figure IV.16 Load-displacement curve in the initial phase of the fatigue test of the specimen M6T1(B). 47
Figure IV.17 Load-displacement curve at 252,342 cycles of the fatigue life of the specimen M6T1(B). 47
Figure IV.18 Load-displacement curve at the final phase of the fatigue test (565,249 cycles) of the specimen M6T1(B). 48
Figure IV.19 Displacement-Total cycles curve registered the fatigue life of 565,249 cycles of the specimen M6T1(B). 48
Figure IV.20 Load-displacement curve at the final phase of the fatigue life (289,398 cycles) of the specimen M6T1(A). 49
Figure IV.21 Displacement-Total cycles curve registered the fatigue life of 289,398 cycles of the specimen M6T1(A). 50
Figure IV.22 Load-displacement curve at the final phase of the fatigue life (52,040 cycles) of the specimen M6T2(C). 50
Figure IV.23 Displacement - Total cycles curve registered the fatigue life of 52,040 cycles of the specimen M6T2(C). 51

List of tables

Table II.1 Minimum number of specimens for testing. 15
Table III.1 Adhesive mechanical properties. 22
Table III.2 The fatigue test program. 29
Table IV.1 Surface roughness parameters. 32

Notations and abbreviations

Notations

G_{max} − Maximum crack propagation energy release rate

G_{th} – Fatigue threshold crack propagation energy release rate

$G_{c(s)}$ – Steady-state energy release rate

$G_{c(i)}$ – Strain energy release rate for crack initiation

f_r − Frequency of cyclic loading

N_f − Number of cycles to failure

E − Elastic Young's modulus

σ − Stress variable

σ_e −Endurance limit

σ_u − Ultimate strength

σ_{min} − Minimum cyclic stress

σ_{max} − Maximum cyclic stress

σ_{eq} − Equivalent static strength

σ_a − Stress amplitude

R_σ − Stress ratio

LR − Load ratio

P_{max} − Maximum cyclic load

P_{min} − Minimum cyclic load

S-N – Stress-Life curve

e-N – Strain-Life curve

Abbreviations

ASTM − American Society for Testing and Materials

DCB − Double Cantilever Beam

DLJ − Double Lap Joint

DLS – Double Lap Shear

ESS − Equivalent static strength

FCG − Fatigue Crack Growth

G – Gibbs energy (Helmholtz energy)

HCF − High-Cycle Fatigue

LCF − Low-Cycle Fatigue

LEFM − Linear Elastic Fracture Mechanics

PMC – Polymer Matrix Composite

T-C − Tension-Compression

T-T − Tension- Tension

SLJ – Single Lap Joint

VA − Variable Amplitude

UCL − Ultimate Compressive Load

UCS − Ultimate Compressive Stress

UTL − Ultimate Tensile Load

UTS − Ultimate Tensile Stress

I. Introduction

Adhesive bonding is a modern technology that allows to join two substrates through the intermediate material – adhesive, and establish strong contact between them. This technology is good alternative to conventional joint technology.

The adhesion plays an important role in various complex structures that require adhesive joining from high technology industries such as aeronautics, aerospace, electronics, and automotive, to traditional industries such as construction, sports, health and packaging, as a result of time and cost saving, high corrosion and fatigue resistance, crack retardance, good damping characteristics. Adhesives have also been introduced in such areas as dentistry and surgery. As the adhesive bonding technology provides the lighter and cheaper alternatives, both the automotive and the aerospace industries have investigated adhesives and associated adhesion mechanism for more 50 years. Nowadays adhesive joints have been studied for the application even in naval industry. This fact emphasizes the importance of research in this challenge area, which influences the quality, reliability and the service life of adhesive bonding. Besides the increasing of utilization of adhesive bonding in structural applications of high technological industries stimulates the growing interest of the scientific community for the study of fatigue behavior of bonded structures. This is particularly true for industrial applications, where the adhesive bonding must be highly reliable. This means that fatigue resistance of adhesive bonding needs more rigorous study.

Although the study of adhesion mechanisms can be traced back to the 1930s, the field of adhesion began to create real interest in scientific circles only about 60 years ago. Even though considerable research has been carried out since then, the fundamental knowledge about adhesion mechanisms is still not well investigated and no single global theory or model can explain all the associated phenomena. This is mainly due to the fact that adhesion is a very complex phenomenon since it involves multidisciplinary knowledge of polymer and surface chemistry, fracture mechanics, materials, rheology and other subjects.

For many adhesively bonded joins used in structural components the dynamic loading is the most important type of loading, defining its service life. In a dynamic loading regime, a structure may fail even inside the elastic phase. Consequently, it is important to estimate the fatigue strength of bonded joints. Among the numerous adhesives, the epoxy resins have many advantages as: bulk, surface properties, low cost and good mechanical properties.

The objective of this experimental study is to investigate, quantify and compare the effect of different mechanical treatment of the mild steel substrates on high-cycle fatigue life of epoxy bonded joints under mode II loading. Three different substrate mechanical treatments were used in present study: bristle blasting, as the most common in industry, grit blasting and

sand blasting. The main goal of this work is to extend the previous studies on analyzing of the influence of substrate roughness on bonded joint strength.

The dissertation contains a complete review of twelve studies of the last 6 years related to fatigue and crack propagation in bonded joints, substrate mechanical and chemical treatment, substrate roughness and its influence on joint resistance. The objective of the review is to provide a learning material and to introduce to the reader the concerns of modern bonding that scientific community carries out presently.

II. General aspects of structural bonding.

Adhesive bonding technology offers great design flexibility as it can be easily integrated into almost all available industrial sequences of single-piece work or mass production. Historically, bonding has long been recognized as a high-performance joining technique. Adhesive bonding is characterized by numerous well-known advantages, such as:

- The adherents are not affected by heat
- Uniform stress distribution
- Vibration damping
- Possibility to join large surfaces
- Possibility of bonding very small elements,
- Possibility to join different materials
- Possibility to join very thin adherents
- Possibility of simultaneous joining and sealing of structures
- Gas-proof and liquid-tight
- No crevice corrosion
- No contact corrosion
- No precise fits of the adherent surfaces are necessary
- Good damping properties
- High dynamic strength
- Electrochemical insulation of elements joined, protection against the formation of electrochemical corrosive cells
- Elimination of negative effect of heat on the properties and structure of elements joined as is the case with welding, spot welding, or soldering,
- ease of modification of adhesives, both physical and chemical, which permits the obtainment of desired physicochemical properties of the bond formed,
- Possibility of creating bonds under highly specific conditions, e.g. in field conditions, under water, etc.
- Possibility of creating bonds using simple equipment, which provides significant reductions in costs.
- Possibility to bond process automatization

Among the factors that restrict the application of the technology:

- Limited stability to heat and humidity
- Long-term use may alter the properties of the bond-line
- Cleaning and surface preparation of the adherents is necessary in many cases
- Specific production requirements to be met

- Specific clamping devices are often required to fix the joint
- Nondestructive quality testing is only possible to a certain extent
- Low resistance to wrench and cleavage strength
- The high sensitivity of the physical properties of adhesive bonds to deviations from the recommended technology,
- Non-linear relation of the strength of adhesive bonds with the size of the surface area of bonding,

These, however, do not significantly reduce the applicability of adhesive bonding.

II.1. Adhesion theories

Adhesion is the interatomic and intermolecular interaction at the interface of two surfaces. Adhesion is a multi-disciplinary topic which includes surface chemistry, physics, rheology, polymer chemistry, mechanics of materials, polymer physics and other. Basically, adhesively bonded joint consists in two substrates – adherends and adhesive layer. Surface roughness often shortened to roughness, is a component of surface texture.

There are four main mechanisms that could explain the adhesion process. According to DA SILVA, L. F. M., *et al*., (2007) these theories are:

- Mechanical interlocking theory
- Electronic (electrostatic) theory
- Adsorption theory
- Diffusion theory

The mechanical interlocking model is one of the earliest theories. It was introduced by MacBain in 1925. The theory proposes the mechanical keying of the adhesive into the irregularities of the adhered surface. The roughness and porosity of substrates are generally suitable factors only in so far as the wettability of the adhesive is sufficient. The non-wetting of substrate's surface can prohibit adhesive bonds from forming at all. Therefore, for strong adhesion the adhesive must not only wet the substrate but also have the proper rheological characteristics for penetrating into pores in a reasonable time. Low adhesive viscosity promotes greater interfacial strength due to its faster and more complete penetration into the micro voids and pores. Despite its obvious appeal, the model of the mechanical interlocking cannot be considered as a universal adhesion theory because good adhesion can occur even between perfectly smooth substrates. Moreover, this theory does not consider any factors that occur on the molecular level at the adhesive/substrate interface. Mechanical interlocking can be effectively applied when the substrates are impermeable to the adhesive and the surface of the substrate is sufficiently rough.

The absorption theory states that the materials will adhere because of the interatomic and intermolecular forces that are established between the atoms and molecules in the

surfaces of the adhesive and the substrate after their intimate contact. These forces include Van der Waals forces, hydrogen forces, covalent, ionic, metallic and donor-acceptor interactions. This theory assumes that an adhesive must wet the surface to be bond (adherends) and led to the development of materials with lower surface tension than that of the adherend. Supporting this theory is the fact that epoxy wets steel and provides a good bond, whereas it does not wet the olefins and does not bond them.

The diffusion theory assets as adhesion as being the result of interdiffusion of the macromolecules of two polymeric materials at the interface. The interdiffusion forms a transition zone or interface. According to the diffusion theory both the adhesive and substrate must be polymers, which are mutually miscible and compatible. In the case of polymer diffusion (autohesion), two samples of identical polymers under a constant assembly pressure, is a function of temperature and contact time. Using this theory can explain the phenomenon of adhesion that occurs between polymeric materials, plastic welding, plastic binding with adhesives, etc.

The electrostatic attraction theory postulates that an electrostatically charged double layer of ions develops at the interface. In another words, forces of attraction occur between two surfaces when one surface carries a net positive charge and the other surface a net negative charge as in the case of acid-base interactions and ionic bonding. The fact that electrical discharges are observed when as adhesive is peeled from a substrate is cited as evidence of these attractive forces. A difference in electrostatic charge between constituents at the interface contributes to the attraction bonding. The strength of the interface will depend on the charge density. The bonding of this type will explain why silane finishes are especially effective for certain acidic or neutral reinforcements like glass, silica and alumina.

II.2. Surface tension or surface free energy

Any adherent surface has surface free energy, that is excess of energy on the surface which appears as a result of unbalance between the forces on the bulk molecule and the surface molecule (Fig. II.1). This effect also can be defined as the energy necessary to form a unit area of new surface or the energy necessary to move a molecule from the bulk to the surface. Surface free energy is expressed per unit area. It can be defined in terms of Gibbs G or Helmholtz free energies. Distinction is also drawn between the surface energy and the surface tension, although they are numerically the same but have different dimensions. In adhesion science and technology the interest is always in complex solid surface where very precise measurements of surface free energy are not generally possible. Surface energies of liquids can be measured by the Du Nouy ring and Wilhelmy plate.

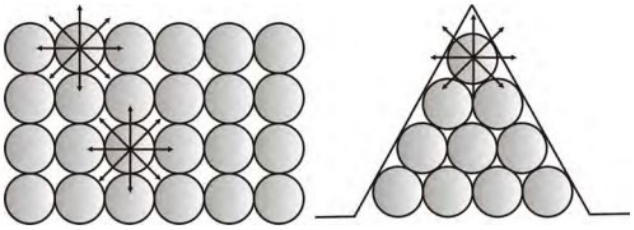


Figure II.1 Intermolecular forces. DA SILVA *et al*. (2007).

The formation a drop of liquid on the solid surface can be described by the equilibrium angle θ, that interprets the equilibrium balance of forces at the contact between three material phases. The relationship between the surface free energies is represented by Young's equation:

$$\gamma_{SV} = \gamma_{SL} + \gamma_{LV} \cos\theta \qquad \text{(II.1)}$$

where γ_{SV} is the surface free energy of a solid substrate (J/m²), γ_{SL} is the surface free energy of a liquid drop (or the surface tension of the liquid), γ_{LV} is the interfacial free energy between the solid substrate and the liquid drop, and θ is the wetting (Young-Dupre) or contact angle between the solid-liquid interface, Fig. II.2.

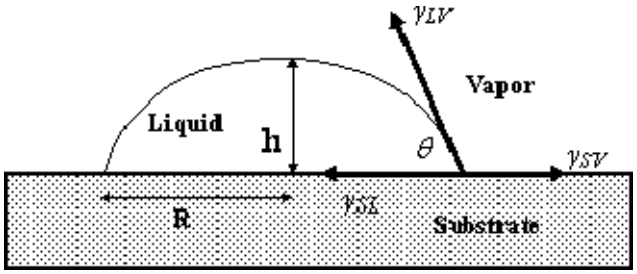


Figure II.2 The illustration of the equilibrium force balance according to Young's equation. Available in: < http://www.jpbsonline.org/article.asp?issn=0975-7406;year=2011;volume=3;issue=1;spage=89;epage=100;aulast=Shaikh>

For wetting to occur spontaneously, the next condition should apply:

$$\gamma_{SV} \geq \gamma_{SL} + \gamma_{LV} \qquad \text{(II.2)}$$

if the γ_{SL} is not significant, this criterion can be simplified:

$$\gamma_{SV} \geq \gamma_{LV} \qquad \text{(II.3)}$$

The last equation indicates that the adhesive will spread on the substrate when the surface free of the substrate is greater than of the adhesive. Poor wetting causes less contact area between the substrate and the adhesive and less stress regions at the interface, and consequently adhesive joint strength decreases.

The value of θ can vary from 0° to 180°. In some samples where the solid substrate has a surface energy much higher than the liquid, cosθ approaches 1 as the contact angle

approaching 0, denoting that the liquid spreads on the substrate's surface. When the solid has a much lower surface energy than the liquid, cosθ approaches -1 as the contact angle approaches 180° and the liquid approaches completely non-wetting state, as shown at figure II.3.

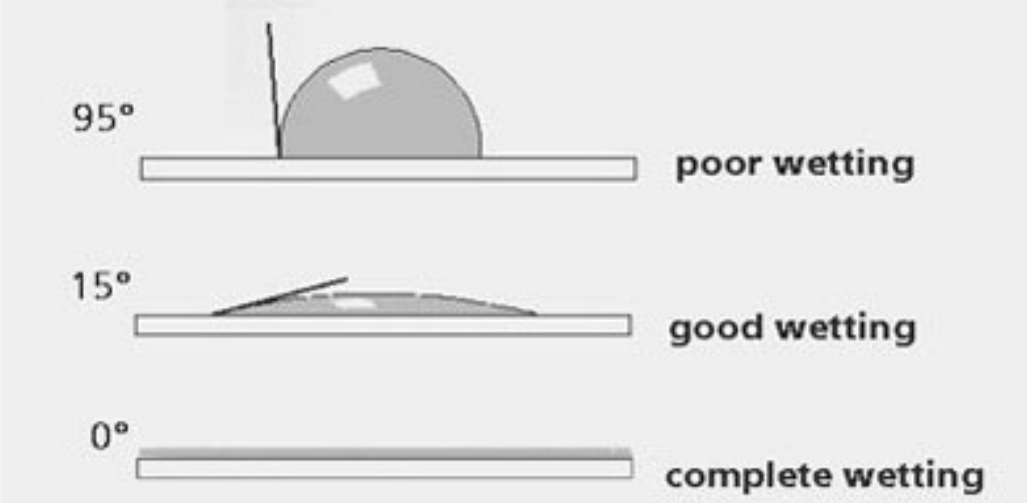


Figure II.3 Liquid drop on solid surface. Available in: < https://www.teachengineering.org/view_lesson.php?url=collection/duk_/lessons/duk_surfacetensionunit_lessons/duk_surfacetensionunit_less3.xml>

The condition θ<90° indicates that the solid is wet by the liquid, and θ > 90° indicates poor wetting, with the limits θ = 0 and θ =180°defining complete wetting and complete non-wetting, respectively.

Considerations of surface energies are usually regarded as fundamental to an understanding of adhesion. Surface free energies are also associated with failure of an adhesive bond. Failure involves forming new surfaces and the appropriate surface free energies have to be provided. The surface free energy term may be the ***work of adhesion, Wa*** or the ***work of cohesion, Wc***, depending on whether the failure is adhesive or cohesive. These are defined as follows:

$$Wa = \gamma_{sv} + \gamma_{lv} - \gamma_{sl} \tag{II.4}$$

$$Wc = 2\,\gamma_{sv} \tag{II.5}$$

Wa is defined as the work needed to isolate the liquid and solid phases, or the negative free energy related to the adhesion of the liquid and solid phases. Work of adhesion is utilized to express the strength of the interaction between the liquid and solid phases. Work of cohesive is defined as the work needed to isolate a liquid into two parts, and is a measure of the strength of molecular interactions within the liquid. The illustration of adhesive and cohesive forces is demonstrated at Fig. II.4.

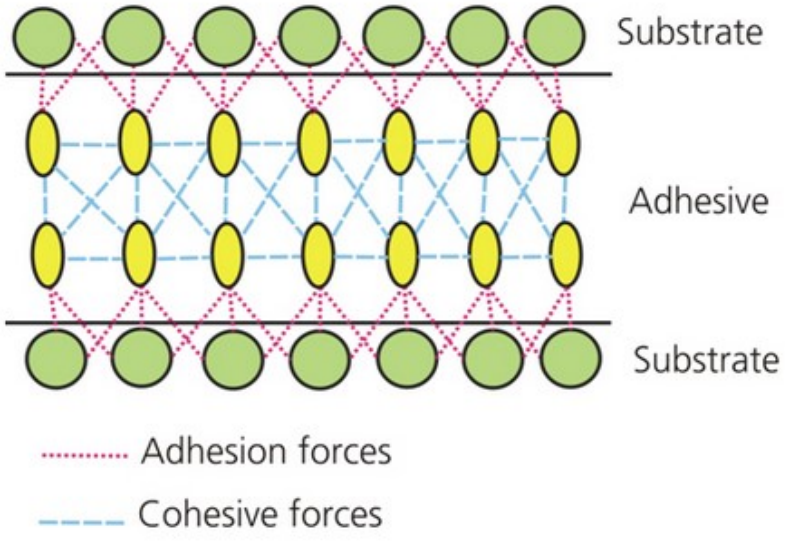


Figure II.4 The illustration of cohesive and adhesive force actuation in adhesive layer. Available in: < http://www.adhesives.org/adhesives-sealants/science-of-adhesion/adhesion-cohesion>

The effect of surface roughness on wettability have been studied by many researchers using surface roughness factors. This was first appreciated by Wenzel (DA SILVA *et al*. (2007)), using a geometrical argument based on the roughness factor, r, the ratio between the actual surface area and the apparent surface area of a rough surface.

A drop placed on a rough surface will spread until it finds its equilibrium configuration, characterized by a contact angle θ* (possibly different from the Young angle θ). The key assumption of the model is sketched in Fig. II.5. As the contact line progresses on the dry solid, it is assumed to follow all the topological variations of the material so that each piece of liquid/air interface replaced by a solid/liquid interface of the same surface area.

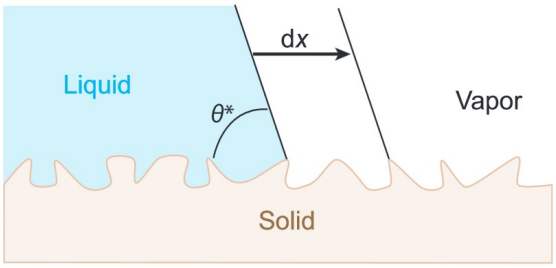


Figure II.5 The Illustration of Wenzel wetting theory.

The surface energy variation dE arising from an apparent displacement dx of the line can be written, per unit length of the contact line, as

$$\mathrm{d}E = r(\gamma_{\mathrm{SL}} - \gamma_{\mathrm{SA}})\,\mathrm{d}x + \gamma\,\mathrm{d}x\,\cos\theta^* \qquad \text{(II.6)}$$

where the second term on the right corresponds to the change of liquid/vapor surface area as the drop spreads. The roughness increases both the solid energies, enhanced geometrically by a factor r. The minimum of E(dE=0) yields if the solid is flat (r=1); if not, it generates:

$$\cos\theta^* = r\cos\theta \qquad \text{(II.7)}$$

where θ is the chemical angle given by Young-Dupre Equation. The Wenzel relation predicts that roughness enhances wettability. If the factor r is larger than 1, a hydrophilic solid (θ < 90°) becomes more hydrophilic when rough (θ* < θ). Conversely, a hydrophobic solid (θ > 90°) shows increased hydrophobicity (θ* > θ). Although these tendencies are generally (but not always) observed, this theory is not quantitative. It can be seen that the Wenzel relation implies strange features. For example, there is no limitation for the effect: the roughness factor can be made arbitrarily large, which seems to imply that complete wetting (cos θ * >1) or complete drying (cos θ * < −1) should be induced by large roughness. Such behavior is not observed because Wenzel assumptions often are not satisfied.

Generally, the surface energy of solids is a function of the following major factors (KUCZMASZEWSKI, (2006)):

$$Ep = f(S, \sigma_n, P, H) \qquad \text{(II.8)}$$

where: S – actual surface and its topographic and chemical features, σ_n – natural stresses in the surface layer, P– tensile strength, H - hardness.

II.3. Roughness

The value of mechanical adhesion is constituted primarily by the topography of surface. The stereo metric parameters of the surface layer play a significant role in the process of adhesive joining of elements. This follows not only from the fact of increase of the actual surface area through its mechanical ”development”, but also results from changes in the degree of imbalance of intermolecular forces in the outer nano layer of atoms and molecules. Surface finish parameters are used in order to evaluate surface roughness quality. The most important and significant of them are: Ra, Rt. Thus, Ra is the arithmetic average of the absolute values of the roughness profile ordinates. Also known, as Arithmetic Average (AA) or Center Line Average (CLA). The average roughness is the area between the roughness profile and its mean line, or the integral of the absolute value of the roughness profile height over the evaluation length, Fig. II.6.

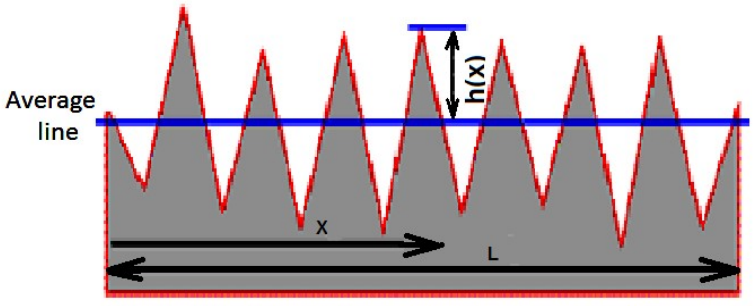


Figure II.6 Average surface roughness, Ra.

The formula for calculation of Ra:

$$R_a = 1/L \int_0^L | h(x) | dx \quad \text{(II.9)}$$

where, h(x) is a height of surface profile, x is a number of points, and L is a length of sample.

R_t is maximum height of the profile, i.e. the sum of the height of the highest peaks and the lowest valley depth within a sampling length. R_t can be calculated as:

$$R_t = R_p + R_v \quad \text{(II.10)}$$

where R_v is maximum valley depth:

$$R_v = min\ hi \quad \text{(II.11)}$$

and R_p is maximum peak height:

$$R_p = max\ hi \quad \text{(II.12)}$$

Consequently, the major values of R_a and R_t evidences the presence of the significant picks and valleys on the surface, which contribute better to mechanical interlocking adhesion mechanism. However, two essentially different rough surface can be present with the same R_a, R_t values. In this case complementary roughness parameters as R_{sk}, R_{ku} should be considered. R_{sk} is the skewness parameter, that represent if the surface has predominantly picks or valleys or an equilibration of them. In the last case the value of R_{sk} would be about 0, the positive value characterizes the majority of picks, a negative value, the majority of valleys. Such surface facilitates a liquid retention and wettability, but tends to have more contaminations and complicates cleaning. R_{ku} is the *Kurtosis* parameter that evaluates the degree of pickiness/flatness of the surface. Thus, flatter surface has negative value of K_{ku} (platycurtic distribution). Picked surface has positive value of K_{ku} (leptokurtic distribution). The surface with $K_{ku} > 3$ tends to accumulate the liquids better, as well as contaminations.

Another surface parameter R_z based on the five highest peaks and lowest valleys depth over the entire sampling length. The calculation formula is:

$$R_z = 1/5 \sum Rpi - Rvi \quad \text{(II.13)}$$

where R_{pi} and R_{vi} are the i–th highest peak, and the I–th lowest valley respectively.

II.4. Weak boundary layer

The relationship between roughness and adhesion is not simple. Optimum surface profile varies from one adhesive to another. It depends on viscosity of the adhesive. In the study BIKERMAN (1961) the author states that when a liquid advances into a surface topographical valley, the air initially present there can escape without experiencing any serious

resistance. If the spreading liquid adhesive covers a surface crevice without penetration and forms air pockets, the surface forces usually cease to affect the position or motion of this air pocket. For efficient bonding, care must be taken to ensure that the adhesive makes intimate contact with the adherent surface. The surface roughness can affect the spreading of the adhesive, either because the adhesive cannot penetrate the adherent or because it gels before the penetration completes. Based on these facts the theory of ***weak boundary layer*** was formulated. It holds that for an adhesive to perform satisfactory, the weak boundary layer should be eliminated. Figure II.7 illustrates graphically classes of weak boundary layers. The weak boundary layer can formed by air pores, impurities, lubricants, additives, adsorption of oily contaminants from the environment, or chemical reactions such as oxidative degradation of the adhesive catalyzed by an ingredient on the metal surface.

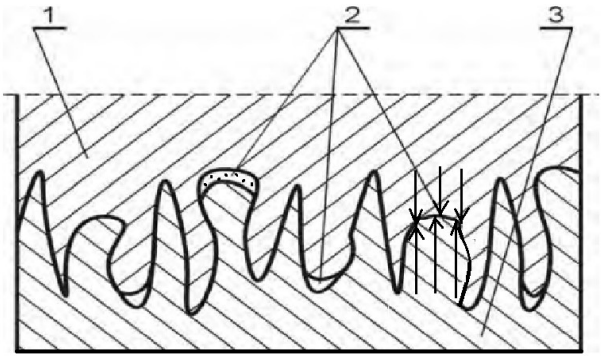


Figure II.7 The Illustration of weak boundary layer: 1 – adhesive, 2 – impurities, entrapped air, chemical reactions, 3– adherent.

Logically, the adhesive bond will fracture at its weakest link. Thus, if a cohesively weak layer exist at the interface, the adhesive bond may fracture within this weak boundary at a relatively low applied stress. Such a weak boundary layer is often very thin, and the fracture may be mistaken with interfacial failure. BIKERMAN (1961) emphasized the role of the weak boundary layer and proposed that practically all cases of weak adhesive strength and all cases of apparent interfacial failure are due to the existence of weak boundary layers. Bikerman model is simple, but was criticized in the past. It is now, however, admitted that many cases of poor adhesion can be attributed to this weak interfacial layer, especially for metal adherents.

As weak boundary layer provokes the failures of bonded joints there are three types of failure in bonded joints: adhesive failure, cohesive failure and mixed cohesive-adhesive failure. The type of the failure that occurs in an adhesive will depend on the forces that act between two substrates. Thus, if the adhesive force is greater than the cohesive, the failure would be cohesive:

$$F_a > F_c \qquad \text{(II.14)}$$

Cohesive failure is obtained if a crack propagates in the bulk polymer which constitutes the adhesive. In this case the surfaces of both adherends after debonding will be covered by

fractured adhesive. The crack may propagate in the center of the layer or near an interface. For this last case, the cohesive fracture can be said to be “cohesive near the interface”. Cohesive failure is the “right” failure in term of joint fabrication. The condition for structural bonded joint design:

$$F_a \geq F_c \tag{II.15}$$

Fig. II.8 presents the illustration of types of failures. When the cohesive force is greater than the adhesive the ***adhesive failure*** occurs. In this case the fracture would be between the adherent and the adhesive layer:

$$F_a < F_c \tag{II.16}$$

Adhesive failure can evidence about the presence of weak boundary layer in bonded joint or about improperly fabricated joint. ***Mixed adhesive-cohesive failure*** is also possible. This is when areas with adhesive and cohesive types of failure are presented in the failure locus.

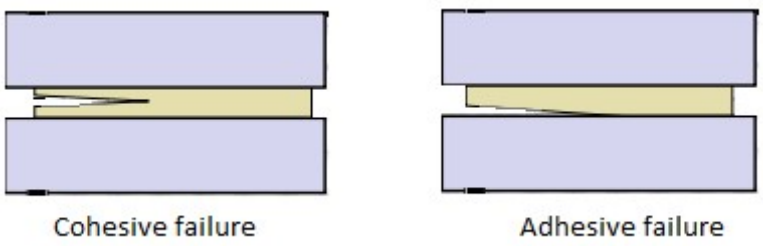


Figure II.8 Types of failure interface.

Many studies have showed that the adequate surface preparation of bonded parts results in a increase of bonding strength. Therefore, to obtain right and tenacious joint it is important to have a careful surface treatment, and this is one of the most important operation in the bonding processes. If the surface preparation is insufficient the bonded joint can breaks down unpredictably, causing adhesive failure. With the right surface preparation the failure will be always cohesive. Surface preparation of the substrates has the target to reach the maximal surface wettability of the chosen adhesive. The surface wettability depends on the surface energy and on the surface integrity, which is related by the surface roughness. The more the bonded surface participates in the adhesive process the higher is the bonded joint strength. This means that the greater roughness creates a better surface for the connection. However the more detailed analyses indicate that the roughness process can start the physical-chemical changes, which influence the surface energy and wettability. Conforming to this statement, at the surface with higher values of roughness parameters the increase in the surface area can lead to a relative increase of adhesion as long as the surface roughness does not lower the contact between surfaces. At adherents the surface energy influences the liquid running over the surface. In this way the surface wetting occurs. For optimal surface wetting, the surface energy of the adhesive (E_a) must be lower than of the substrates (E_s) i.e.:

$$E_s > E_a \quad \text{(II.17)}$$

The degree of the adherent surface coverage by the adhesive depends on its viscosity, on the surface cleanliness, on the surface asperity form and on the adhesive curing time. An adhesive application must be sufficiently slow to permit the asperities filling in comparison with the time necessary to adhesive curing.

II.5. Surface treatment

Basically there are two types of mechanical surface preparation, namely of abrasive and erosive wears. In both cases the knurling and cutting of material occurs. The abrasive wear is typical of the mechanical preparation using grinding methods. The grinding proceeds cutting a big number of grains of irregular geometry and can be obtained by using hard particles. From the abrasion theory follows the possibility of a surface roughness change at the influence of load and path length change at the manual grinding. The erosive wear is typical characteristic of surfaces that have mechanical preparation usually obtained by blasting. Logically, the impact particle energy must be sufficient and the impact angle must be right for the replacement and detachment of material from the surface occurrence. The surface that has erosive wear represents rippling and corrugated appearance.

The manner of surface preparation for adhesive bonding is different for different materials. For carbon steels there is, as rule, surface cleaning, mechanical “development” of surface (e.g. through sand blasting or roughing up with abrasive paper, etc.) and degreasing. For alloy steels, aluminum alloys or titanium alloys appropriate chemical treatments, rinsing and drying are required to obtain good quality bonds. The primary objectives of the preparation of surface layer of bonded elements are as follows:

- removal of inorganic contaminants from the surface,
- thorough degreasing of the surface,
- possible activation, i.e. special treatment aimed at increasing the value of free surface energy.

The more important methods of constituting the adhesive properties of the surface layer are as follows:

- mechanical methods (machining),
- chemical methods,
- activation by means of corona discharges,
- oxidation with ozone,
- activation by means of partial discharges,
- flame activation,
- activation by means of high-energy plasma, high-energy electron beam,
- activation by means of UV radiation,

- others, e.g. combinations of mechanical and chemical methods.

Machining is applied mainly in the process of preparation for joining elements of carbon structural steels. Its objective is to remove iron oxides, since they are weakly bound with the substrate, and also to partially "develop" the surface. Typical methods of machining used in processes of surface preparation for adhesive bonding include grinding, blasting, etc.

Blasting is a good method for machining of large surfaces. Blasting is the process where small angular or spherical particles are propelled at a part by compressed air, or mechanical high speed rotating wheels or water pumps. The blast media type, shape, size, density, and hardness, along with media acceleration and volume of media, combined with standoff distance from the workpiece, angle of impact and time cycles are important factors in the blast process capabilities. Moreover authors as HARRIS *et alli*. (1999) emphasize that the fine differences in the blasted grains types and size results in a measurable change on the surface characteristics. The authors CHANDER *et al*. (2009) confirmed that the coarse abrasive induces rougher surface and generally the more rough surface show the lower surface energies. The influence of even minimal surface treatment on fatigue life of bonded joints was proved experimentally by BERMEJO *et al*. (2008). They observed the increase of resistance for infinite fatigue life of pre-painting joints in 1,7 times.

II.6. Adhesives for metal bonding

Metal bonding is the dominant application in structural components, especially in highly reliable industries. The more important features of a good adhesive for metal bonding can be presented synthetically as follows:

- possibly low viscosity, facilitating wetting,
- relatively low free surface energy,
- presence of various functional groups in the chemical structure of the adhesive, expanding the applicability of the adhesive and permitting the formation of chemical bonds,
- low chemical curing shrinkage rate, in the case of thermal-setting adhesives also low thermal cure shrinkage rate; this permits bonding under contact pressure,
- possibility of curing at ambient temperature,
- short curing time,
- resistance to cracking of brittle character.

A good adhesive for metal bonding should contain as many various functional groups as possible, capable of the processes of chemisorption with the material of the substrate. Its chemical structure should impart to it high cohesive strength as well as elasticity to guarantee good damping properties and ability to "absorb" loads. Functional groups play

a highly significant role in the chemical structure of adhesives. They permit the formation of chemical bonds between the adhesive and the substrate and determine high strength of the joint.

II.7. Fatigue testing parameters for metal bonded joints

Among the numerous different methods for fatigue testing of metal-metal adhesively bonded joints is standard ASTM D3166-12. According to KUZCMASZEWSKI (2006) the minimum number of cycles cannot be less than 2000, the recommended value being 10E7. The mean stress in cycle should be less than or equal to 50% of the static strength, the load ratio should be 0.1, the frequency is 30Hz and sinusoidal loading.

II.8. Minimum number of specimens for fatigue testing

Reliable fatigue results obtained from experimental work must use fatigue standards. In order to realize this contest the standard ASTM E739-91 (2006) Standard “Practice for Statistical Analysis of Linear or Linearized Stress-Life (S-N) and Strain-Life (ε-N) Fatigue Data” recommends the minimum quantity of specimens that should be tested effectively for plotting reliable S-N and ε-N curves. The Table 1 presents the optimal number of specimens for different types of researches.

Table II.1 Minimum number of specimens for testing.

Research	Minimum number of specimens
Preliminary probe testing	6-8
Research and development	6-8
Research for project	12-24
Research of reliable database	12-24

II.9. Review of recent works

Numerous studies were realized on the adhesive field last years. Many of them are related to the fatigue resistance of bonded joints. Besides many works are concern about substrate treatment as a most influence factor in bonded joint quality. A lot of attention is paid to structural epoxy adhesive, due to its good resistance that can be used in highly reliable areas of industry. Thus, the work of THEVENET *et al*. (2013) concerns about the influence of mean load and loading type on the mechanical behavior of a ductile adhesive under monotonic and low-cycle fatigue loading for different loading types, such as shear, tensile, shear-tensile and

shear-compression stresses. Epoxy resin Araldite 420 (Hantsman) and aluminum 2017 substrates were used to manufacture the joints. The tests were performed in end-notched flexure format and under several load amplitudes from 2 to 7 kN, loading rate 1 kN/s, mean load 2-7 kN, loading frequency from 0.035 to 0.125 Hz, at normal environment conditions. The results of the study lead to conclusion that the increase of mean load or amplitude without changing other loading parameters reduces significantly the service life of bonded joint. The cumulative displacement at failure is lower under tensile loading than under shear loading. Thus, the influence of mechanical defects like sample geometry, device position, presence of inclusions in the adhesive is more significant under tensile loading. Behavior under tensile-shear loading was also observed. As can be seen from the results, the amplitude has more significant effect to fatigue life then mean load. Another important conclusion is that the shear behavior mainly controls the tensile-shear behavior of the bonded joint. The cumulative displacement is a little bit lower than those reached under shear loading. The influence of the amplitude on compression-shear fatigue life of bonded joints is major than the mean load. The authors also noticed that the large value of cumulative displacement at failure could be due to the friction loads caused by the compression part of loading.

The authors MENICONI *et al.* (2014) describes the fatigue analysis of composite repair that would be applied to the metallic hull of floating, storage and offloading platform. The main objective of the work is to address the durability and expected operational life of the repair, with emphasis on the adhesive bonded interface metal-composite. The technology that became more popular in Brazil and abroad don't have yet much knowledge about its long term performance when applied to harsh, dynamic applications like naval structures in operation. In order to evaluate the reliability of this modern repair technology they performed some tests end realized numerical simulation, as well. They realized a double lap shear testing (DLS) with a metallic plate of 8 mm thick, 500×650 mm of area, laminated at the one side using the same scheme proposed for the repair, i.e. a first layer of resin, one layer of glass chopped strand mat (CSM), followed by thirteen layers of the non-crimp carbon (fabric composite material with a biaxial 45°/-45°) lamination. The laminated region had 370×650 mm, the thickness of 8 mm. A groove was introduced in the metallic plate to simulate the thickness loss. The tests were performed with the specimens of 25 mm wide and different sizes of overlap. From the DLS testing it was observed that the maximum effective overlap length was around 100 mm, beyond which the unit failure load reaches a plateau value of 736 N/mm and the former defines the critical shear stress of the system of 7.4 MPa. The effect of shear stress on the repair was verified experimentally through three points bending tests on 6 inch I-beams, with and without composite reinforcement. For this the composite patch was applied to the web of the beam, with 45°/-45° fiber alignment for optimal shear reinforcement. Eighteen layers were deployed, resulting in 9.2 mm of structural carbon laminate and a 0.6 mm of adhesive layer. The tests demonstrated the elastic regime between 100 kN and 150 kN. In this interval of load there was

increase in shear stress of 35MPa for the unreinforced beam and an increase of 27 MPa for the reinforced beam. The fatigue testing also was performed with the objective to evaluate the crack propagation rate. The test was realized in the maximum load, with load ratio of 0.1, frequency of 10 Hz, and the temperature control in order to avoid over-heating. The fatigue test displayed the maximum crack propagation energy release rate G_{max} = 317 J/m, that corresponds to the extremely low propagation of 1 ηm per cycle and this means that the defects would practically not grow due to fatigue. Monitoring test was executed with the objective to understand the repair response to the environmental conditions, such as wind, temperature changes, sea state, storms, current loads, etc. To achieve this objective thirteen optical delta strain gage rosettes were applied at the external surface of the composite patch repair of real platform, together with two dummy sensors for temperature compensation. The monitoring test lasted 10 months. From the database of monitoring test it was observed that long term stress ranges sometimes approached the maximum load, but it´s still well below the fatigue threshold. Another result indicates that eventual defects that exist in the metal/composite interface will not grow due to fatigue. The last testing realized by the authors of this study was aging with followed DLS testing in order to address any modification of the interface behavior. To do that, they submitted a part of the original reinforced plate to an accelerated aging program in an environmental chamber, firstly with one week long exposition to salt spray, followed by another week long exposition to UV radiation. This phase lasted for 6 months, and UV exposure was prolonged for more 8 months. At the end of this period there was not any visual indication of degradation of the reinforced plate. The test also demonstrated that the repair itself provided an efficient barrier against the environment and protected the interface from chemical or physical attack. All the tests were executed successfully and had positive results.

The study of MULLER (2011) concerns about the evaluation of the dependence between bonded joint strength and roughness parameters R_a and R_z. The bonded joints were made with epoxy adhesive and constructional carbon steel substrates. Two different mechanical treatments (manual grinding and artificial corundum blasting) were made on the substrates. The treatment was made with identical material structure but different sizes in order to evaluate the influence of different grits on the change of the mechanical preparation. During the investigation the author confirmed the increasing trend of overlap surface, i.e. higher values of bonded joint strength were reached at lower parameter R_a/R_z. Another observation is that the determined roughness parameters Ra and R_z of specimens prepared by different persons are comparable.

DE BARROS *et al*. (2012) investigated experimentally the influence of mechanical and chemical treatment on the adhesion of metallic substrates with geopolymer. To do that it was used carbon steel (A36) and aluminum (6061 alloy) substrates, bonded with geopolymer, based on metakaolin. The substrate surfaces were treated with grit blasting (G40), sand blasting, nitro-phosphoric acid attack and silanization. Combining these four different mechanical and

chemical methods six surface treatments were obtained: grit blasting, grit blasting with followed sinalization, grit blasting with followed acid attack, sand blasting with followed sinalization, sand blasting with followed sinalization, sand blasting with followed acid attack. Five joints were fabricated with each surface treatment and with each kind of metal. Surface analyzing showed that grit blasting mechanical treatment gives greater values of average surface roughness, Ra, than sand blasting, while chemical treatment reduces the same parameter in steel substrates and even more for aluminum ones. Single-lap joints with the adherend size of 103×25×1.2 mm, with the overlap of 12.5 mm, adhesive thickness of 0.5mm were tested under mode II loading. It was observed that the joints failed before any deformation of the substrates. Testing results indicated that the geopolimers developed almost two times higher strength in steel than in aluminum joints for any surface treatment, reaching up to 5 MPa. The bond strength values were slightly lower that it was expected for organic adhesives. Another result obtained from the study was that the chemical post-treatment is not very effective on the strength of steel bonded joints and even more inefficiently for the aluminum joints.

SAHOO *et al*. (2012) investigated the correlations between fracture parameters and the de-bond growth data using both experimental and numerical techniques. Experimental part is related to crack propagation of aluminum-aluminum bonded single lap joints under cyclic loading. Numerical study is concerned about the influence of the pre-crack size on the fatigue life. For the experiments they used aluminum substrates of thickness 1.6 mm, 100 mm length and 25 mm width. The substrates were etched to remove oxides. An adhesive film (Redux-319A) of 0.12 mm thickness was used as adhesive, a pre-defined crack of 3 mm was made at the bond end. The tests were performed applying a sinusoidal load of amplitude 1 kN and stress ratio, R=−1, at the frequency of 1 Hz, at room temperature condition. The de-bond growth data was obtained until the final failure occurs. De-bond was filled with liquid dye-penetrant along the mid bond of the joint as de-bond would be growing. At several stages of its growth, the position of the dye-penetrant was progressively photographed and these stages were marked with the number of cycles of fatigue loading applied till then. The result of the experimental study showed that the crack propagation started between 10^3 and 10^4 cycles, the total failure occurred after 10^4 cycles with cohesive type of locus. For the numerical simulation geometric non-linear finite element analyses was carried out for different de-bond lengths from 3.7 mm to 5.1 mm in steps of 0.2 mm in modes I and II cyclic loading. The result obtained from the numerical simulation for 7 different pre-crack sizes demonstrated the fatigue life between 10^3 and 10^4 cycles. Another result indicated that the adhesive being brittle compared to metallic materials, Paris exponent value obtained is considerably higher and suggest smaller growth lives in such joints.

The development of engineering software allows the modeling and estimation of fatigue life of bonded joints. The researches usually performed experimental test and, then model the specimen behavior in some FEM program, using the results of the experimental test as data

base for FEM. Thus the authors of the work BERNASCONI *et al*. (2010) investigated experimentally the fatigue crack propagation in adhesively bonded, thick composite joints using double cantilever beam and single lap specimens and then compared experimental data with numerical model. For the experiments they used single lap joints, made with composite and steel adherents, with the overlap of 25.4 mm and 50.8mm. Bond line thickness was 0.2 mm consisted with epoxy adhesive 9323B/A (3M). Fatigue testing was performed at room temperature, under mode II loading, cyclic frequency 2Hz, load ratio 0, mean load of 23-31% of ultimate tensile load. During the testing the fatigue crack propagation was monitored by observation of the bond line and surrounding material, using a travelling optical microscope equipped with a digital camera. Pictures were recorded every 500 cycles. It was observed that the crack growth starts from both ends, but after a certain number of cycles one became dominant and finally results the total failure after 10^4 cycles for the specimens tested at mean loading of 31% and 10^5 cycles for 23% respectively. The crack propagation started in the adhesive layer and then continued within the composite material. Fatigue testing also was performed for DCB specimens with similar testing condition. Numerical model was compared with experimental results and evaluated as having relatively good accuracy. In particular the model based on the value of the total energy release rate, G_t allowed the predicting a total number of cycles, whereas the model based on an expression of an equivalent energy release rate G_{eq} combining phases I and II propagation, allowed a more accurate simulation of the initial stage of the propagation only.

Another work is related to the influence of roughness on fatigue life of bonded joints is AZARI *et al*. (2010). The authors tested aluminum (and steel) using an asymmetric double cantilever geometry with the thickness of one substrate doubled in relation to the other one. Epoxy adhesive was used at double cantilever joints with 380 μm of thickness. Five different levels (R_a = 1.3…..9.0 μm) of roughness was obtained by orbital sander and grinder. Fatigue testing was performed at room temperature, at frequency of 20 Hz and load ratio 0.1. The unloading joint compliance approach was used to measure the fatigue crack length. This experimental study proved a significant effect of surface roughness of substrates on fatigue threshold energy release rate, G_{th} under mixed-mode fatigue loading. The minimum G_{th} was measured for the lowest roughness of R_a =1.3 μm, and increased about 50% as the roughness was increased to R_a = 3.9 μm. The maximum value was also measured for R_a = 6.4 μm, then it decreased 20% for a very rough surface of R_a = 9.0 μm. This decrease could be attributed to the increase in stress concentration at the tip of the roughness asperities, and also to void formation resulting from entrapped air and possibly weakly attached asperities. This leads to conclusion about the existence of optimal level of surface roughness. Besides, for fatigue and quasi-static loading under mode I, all the energy release rates (G_{th}, $G_c(s)$, $G_c(i)$) showed no dependency on surface roughness. This is due to the crack path being far from the interface and well within the adhesive.

Extensive study with objective to quantify the various variables affecting the strength of single lap joints under fatigue loading was realized by DA SILVA *et al*. (2009). Effect of material, geometry, surface treatment and environment on the shear strength of single lap joints were investigated using Taguchi method. In their experiments they used three different types of adhesive (very brittle, very ductile and intermediate) and two different substrate material (low strength steel and high strength steel). They tested SLJ with the overlap of 12.5-50 mm, and width of 25mm, and three values of adhesive thickness 0.5-2mm. Surface mechanical treatment was made with #180 sand paper and chemical coating. The roughness obtained was in the scale of 203-305 ηm of R_a parameter and 2228-3301 ηm of R_z parameter. SLJ were tested in pure shear mode. Ageing conditions were 50°C, 80% of humidity, for four weeks period. The results obtained from the study showed that on the mild steel surface treatment provides more irregular and rougher topography that on the hard steel. The factors and their influence on the failure load are follows: the overlap (46% of contribution), when it increases the shear strength increases; the adhesive thickness (19%), as it increases the shear strength decreases; adherent thickness (18%), as it decreases shear strength increases; adherent shear strength (3.8%), as it increases the failure load of joint increases; adhesive toughness (5.5%), when it increases in the range 346-526 N/m the joint strength increases, then decreases to 2902 N/m. The effect of surface treatment, durability and test speed were found negligible.

The understanding of the important role of surface mechanical preparation stimulate the scientific community to study this process. As blasting is one of most popular method of substrate mechanical treatment, authors CHANDER *et al*. (2009) investigated the mechanism of material removal during the blasting of low carbon steel using alumina grits and influence of different blasting parameters. X-ray diffraction and Barkhausen noise analysis technics were used for measuring residual compressive stress on treated surface. The experiments were performed in next conditions: alumina grit size 24–60, blasting pressure 5-7 bar, blasting time 15-180 s, standoff distance 50-200 mm. The influence of blasting parameters are summarized as follow: the roughness increases with the blasting time in the interval from 30-60 s, then it decreases as the time approaches 3 min; the roughness increases with blasting angle up to 80°; a higher blasting pressure results the higher roughness; the roughness increases with standoff distance up to 100 mm; the roughness is higher with bigger grit size. Another results obtained from study indicated that grit blasting produce a surface with a compressive residual stress, moreover the parameters as blasting angle and blasting pressure directly influence the plastic deformation. The authors also identified two mechanisms, namely, micro cutting and indentation (plastic deformation) acting during the blasting process. The compressive residual stress in the blasted layer varies in the range of 282-370 MPa. The hardness is highest at a point nearest to the surface and it decreases with distance from the surface.

The study of BLAND *et al*. (2013) is concerned about the influence of surface pretreatment on fatigue life of aluminum structural joints in liquid water and water vapor environments. The authors tested the joints with three surface pretreatments: grit-blast and degreasing (GBD), phosphoric-acid anodizing (PAA), and PAA followed by the application of an anti-corrosion primer (PAAP). The results reveled that GBD joints was less resistance in water vapor and even less resistance in liquid water comparing with PAA and PAAP joints. The failure locus of GBD joints is predominantly adhesive. The joints with PAA substrates have relatively good durability in both environments. The addition of a primer layer appears to have no significant beneficial effect, but a significant change in terms of the nature of the environment to which they have been exposed. The failure locus of such joints are purely cohesive when they exposure to water vapor. The small changes in the failure locus for PAA and PAAP joints that results from water immersion indicates that adhesive degradation was responsible for inferior durability of joints in the liquid water environment.

The authors SPAGGIARY *et alli.* (2013) investigated the effect of mechanical surface treatment of aluminum and steel joints. Two different adhesives (epoxy resin, acrylic adhesive), two joint geometry (single lap, double lap) and three surface treatments (sand papering, sandblasting and knurling) were employed in the experiments. Untreated substrates also were used as the reference configuration. The results obtained from the study confirmed that the surface treatment is the only variable which affects the joint performance. Thus, the knurled adherents, due to deep indentation, are the roughest ones, but they perform only slightly better than untreated adherents. The fact that knurling doesn´t provide uniform micro patterning, but creates only a number of holes which will be filled by the adhesive explains the minor resistance of the joints with such treatment. Sand papering and sandblasting granted the best performance, promoting a cohesive failure in many cases, especially in the case of steel adherents. Additionally, sand blasted joints have more stable and repeatable results.

Another work that concerns about crack propagation of grit blasted aluminum joints belongs to BUDZIK *et al*. (2014). The authors tested double cantilever beam specimens bonded with epoxy adhesive under monotonic and cyclic loadings (up to 5000 cycles). Dynamic tests were performed under the load corresponding to 50% and 60% of critical fracture energy determined from monotonic test. They observed that the crack started to propagate after 4000 cycles. Back face substrate strain monitoring reveled that crack tip fields for both types of loading were essentially similar. This study corroborated analysis obtained from the Timoshenko beam on Winkler elastic foundation model. The method described in the study was used to validate and calibrate of finite element simulation of crack propagation.

III. Experimental procedure

III.1. Materials and methods

The adhesive joints were made using the plates of low carbon steel A36 and structural intermediate epoxy adhesive NVT, by Novatec S.A., Rio de Janeiro, Brazil. The distinct roughness was applied on the steel plates, before they were cut in specimen size. The joints were manufactured individually in a mold and the adhesive thickness was controlled by the utilization of a dispositive, especially developed in the laboratory. This dispositive guarantees the specimen's dimensions repeatability. The joints were cured in the conditions recommended by manufacturer: at 25ºC, 35 min of application time, 120 min of initial cure time and 24 hours of functional cure time.

The mechanical properties of the adhesive were obtained by the manufacturer in according to ASTM, ASTM D638 (2010), and are shown at Table III.1. The bonded joints were tested statically and at high-cycle fatigue loading in a 100 kN servo-hydraulic machine Instron (Fig. III.1). Specimen installation in servo-hydraulic machine is presented in Fig. III.2.

Table III.1 Adhesive mechanical properties.

Mechanical property	**Value**
Yield strength, σ_{ys}(MPa)	27
Hardness, H, (Shore)	60



Figure III.1 Servo-hydraulic machine Instron 100kN. Available in: < http://www.azom.com/equipment-details.aspx?EquipID=1183>



Figure III.2 Specimen installation in servo-hydraulic machine.

The mechanical properties of the substrate material low carbon steel A36, are σ_{ys} = 250 MPa, σ_u = 400 MPa, according to ASTM A36/A36M - 14. Two blasting machines were used to obtain necessary mechanical roughness in bonding surface: a manual blasting machine IBIX 25 (IBIX), (Fig. III.3) that uses different types of blast material and a bristle blasting machine MBX (MONTI Tools), which uses high-carbon steel wire bristles (Fig. III.4).



Figure III.3 Grit blasting machine. Available in: <http://www.archiproducts.com/pt/produtos/11237/decapagem-limpeza-por-jacto-de-areia-esmerilamento-ibix-25-ibix.html >



Figure III.4 Bristle blasting machine. Available in: <http://www.consumablesexpress.co.uk/mbx-air-op-machine-c-w-3-belts->

Two blast materials were used for roughening the bond surface: garnet sand 20/40 mesh and grit steel G-25 fabricated by Jatofer. The illustration of the grit medias are presented at Fig. III.5 and III.6. Initially the area was degreased with acetone, than blasted in the ways mentioned above and cleaned again with acetone before the application of the adhesive.



Figure III.5 Steel grit GP-25. Available in: < http://sinobestar.sell.everychina.com/p-102514565-cast-steel-grit-g80-0-3mm.html>



Figure III.6 Garnet sand. Available in: < http://www.diytrade.com/china/pd/12067401/Garnet_abrasive_sand_blasting_met

Other dispositives and materials used in experimental study were: stereoscopic loupe (Fig. III.7), fabricated by Metrimpex for measurement of the failure geometry of the tested specimens; water based white paint for painting lateral side of the specimens to make the cracks visible, as shown in Fig. III.8.



Figure III.7 Stereoscopic loupe Metrimpex.



Figure III.8 Bonded joint with painted lateral side.

Surfaces were analyzed in a Taylor Hobson roughness Talyscan 150 fabricated by Leicester, UK (Fig. III.9). This tool is non-contact scanning instrument designed for 3D measurement. It is a dedicated topography system, that scanning a surface of 10 mm x 10 mm with a 2-mm diameter laser probe, in accordance to ISO 4288 (1996).

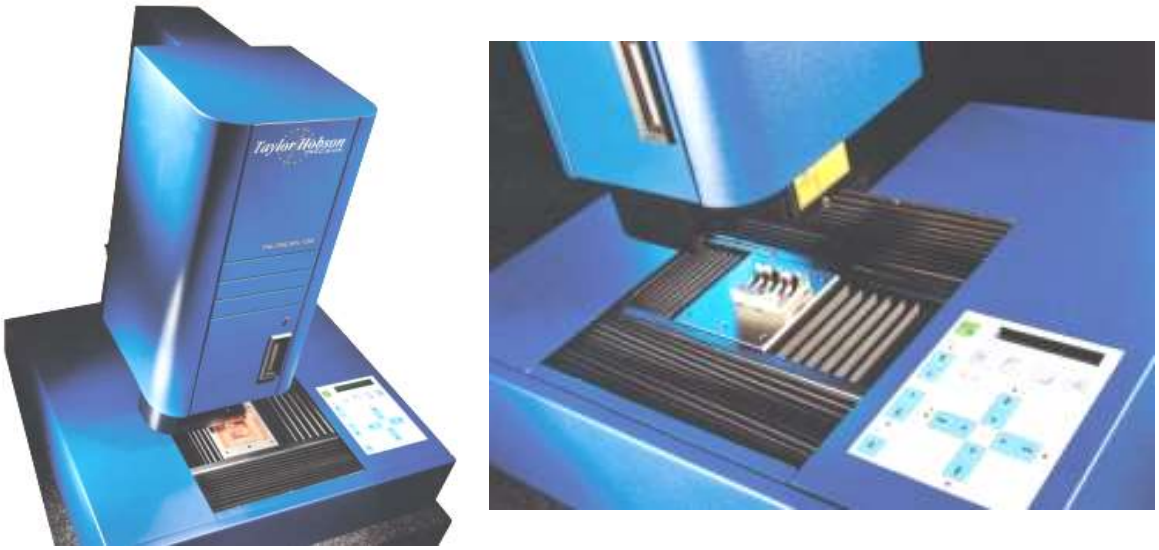


Figure III.9 3D roughness tester Talyscan 150. Available in: < http://www.hoskin.qc.ca/uploadpdf/Instrumentation/Taylor%20Hobson/hoskin_TSCAN150_44ad086f7458b.pdf>

The treated bonded surfaces were analyzed using contact roughness tester Mitutoyo, presented in Fig. III.10 for obtaining the parameters of the surfaces. The scan speed was setted in 1000 μm/s under temperature and humidity control (23°C and 55% RH).



Figure III.10 Contact roughness tester Mitutoyo. Available in: < http://www.lighttoolsupply.com/catalog/Manufacturers/Mitutoyo/Mitutoyo-Surftest-SJ-210-Portable-Surface-Roughness-Tester >

It was used 36 specimens in the experiments. All of them were tested in the same environment conditions. The experiments were realized at room temperature (25ºC) and relative humidity of 55%.

III.2. Monotonic thick adherent shear testing

An alternative approach for determining the shear properties of an adhesive is to apply uniaxial tensile or compressive load to a specimen consisting of thick, rigid adherends, with a short overlap length. This test geometry was developed to overcome the inherent weaknesses of the double-lap shear test. In particular, this method avoids the effect of the specimen extra stiffness of DLS test which makes it more sensitive. Various thick adherend geometries have been suggested, including those specified in ISO 11003:2 and ASTM D 3165. The geometry is used in present study is shown at Fig. III.11.

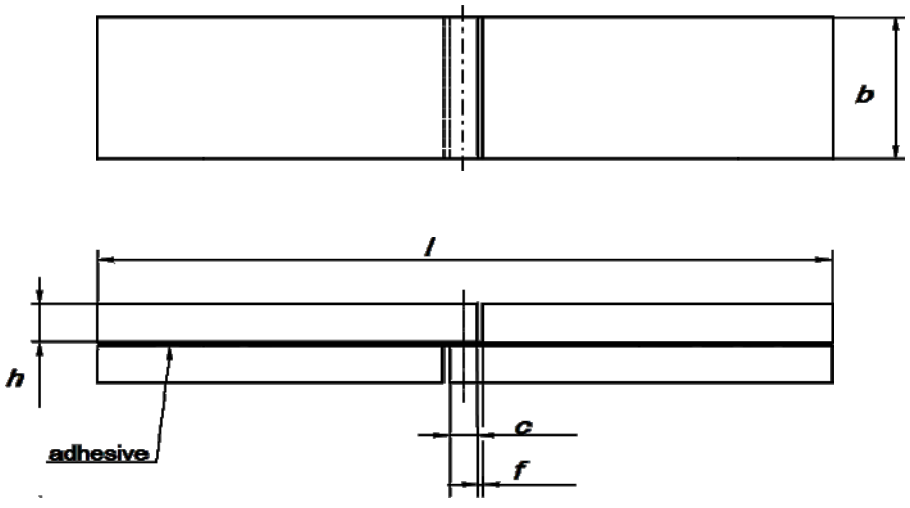


Figure III.11 Specimen dimension and configuration for TAST.

Substrate dimensions can be resumed as length, l = 110 mm, width, b = 25 mm, thickness, h = 6 mm. The adhesive thickness stablished was 0.5 mm, the length of the bonded area, c = 5 mm, the slot width, f = 1.5 mm.

For thick adherent shear testing (TAST) the specimens can be produced by one of two methods:

- Bonding two pre-shaped bars together; or
- Bonding two sheets together and then milling two parallel slots.

The advantages of TAST method:

- Possibility of determination of yields shear strength and shear modulus;
- Compatible with all metals, plastics and PMCs;
- Stress state relatively uniform over bondline;
- Straightforward/economic (moderate cost);
- Simple specimen fabrication and testing
- Simple data reduction.

Disadvantages of TAST method:

- Complex/expensive extensometers (2 off) required;
- Special bonding fixture required;
- Accurate specimen machining required;
- Stress concentrations present at bondline ends;
- Complex analysis;
- Limited fatigue capability.

The objective of TAST method in present study was comparing the resistance of the bonded joints with different substrates roughness to quasi-static loading with the resistance to fatigue loading. Twelve specimens were fabricated bonding two sheets together and then milling two parallel slots. The specimens of each mechanical treatment were tested with the test geometry according to ISO 11000:2 for bonded adherends. The illustrations of specimen configuration and position in testing dispositive are presented in Fig. III.12.



Figure III.12 Position of the TAST specimen in testing dispositive.

III.3. Monotonic end-notched flexure testing

Monotonic end-notched flexure (ENF) tests were performed in order to determine maximum load of dynamic test program. The distance between the specimen supports was 2L = 160 mm. The length of pre-crack was stablished as a_0 = 25 mm. The substrate dimensions can be resumed as length, l = 190 mm, width of 25 mm, thickness, h = 6 mm, adhesive thickness is 0.5 mm. The illustration of the specimen's geometry is shown at Fig.III.13.

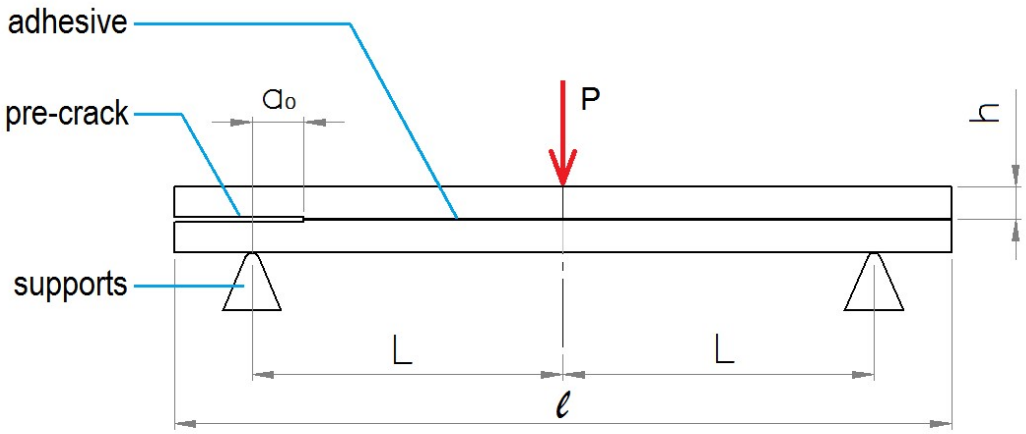


Figure III.13 End-notched flexure joint dimension and configuration.

End-notched flexure format was used as a most appropriate test for mode II fracture characterization of bonded joints. Under this type of loading the substrates is exposed to bending moment while the adhesive is submitted to pure shear loading. Monotonic tests were executed at a crosshead speed of 3 mm/min. The load-displacement curves were registered during the test.

III.4. Dynamic end-notched flexure testing.

Fatigue tests were performed in four different loading levels, in the range of 50-80% of maximum strength, obtained from static test. Sinusoidal loading waveform with a frequency of 20Hz and loading ratio, $R = P_{min}/P_{max} = 0.1$ were used for fatigue tests, see the Table III.2. Thus the maximum fatigue load, P_{max} for each level is proportional to this maximum static load. The load amplitude, P_{amp}, and average load, P_{avr} were calculated using classic fatigue expressions. The loading amplitude, P_a was calculated with the purpose of setup the test machine. The fatigue experimental program was designed to derive experimental data that cover the entire lifetime between 10^2 cycles and 10^6cycles. The specimens were labeled accordingly, e.g. M8T3(A) represents the third specimen with grit blasting mechanical treatment loaded at a level of 80% of the ultimate tensile load. At least three specimens were tested at each load level in order to also obtain information regarding the scatter of the fatigue life.

Table III.2 The fatigue test program.

Level	Maximum load, (%)	P_{max} (kN)	P_{min} (kN)	P_{amp} (kN)	P_{avr} (kN)	R
1	50	3.15	0.315	1.416	1.731	0.10
2	60	3.78	0.378	1.699	2.077	0.10
3	70	4.41	0.441	1.982	2.423	0.10
4	80	5.03	0.503	2.265	2.769	0.10

The specimens have been tested until failure occurred or until the number of load cycles passed 10^6 cycles, which is considered infinite life. Dynamic tests were performed under load control. The load-displacement, displacement-time, load-time and displacement-cycles graphics have been recorded during the test in order to control the right execution all of the test parameters by testing machine. Thus, the load-displacement graphic shows the displacement of the specimen midpoint in function of the load. The negative values of displacement are due to the machine displacement orientation. As can be seen at Fig. III.14 from the graphic the displacement of the specimen was approximately 0.4 mm. Fig. III.15 is shown the load-displacement graphic of the last cycles of specimen fatigue life.

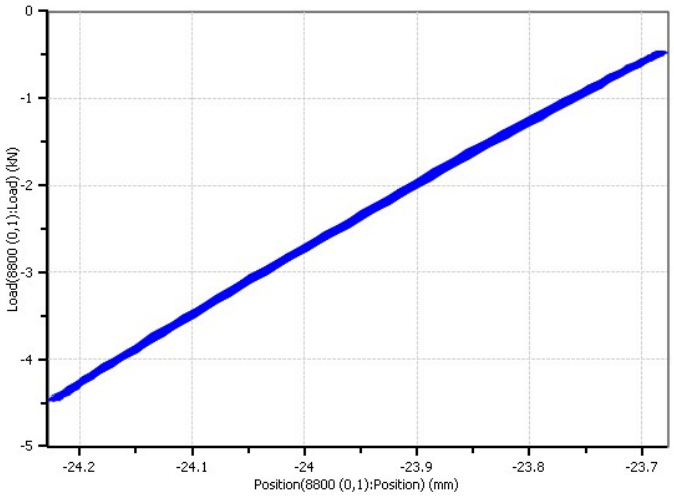


Figure III.14 Typical load-displacement graphic.

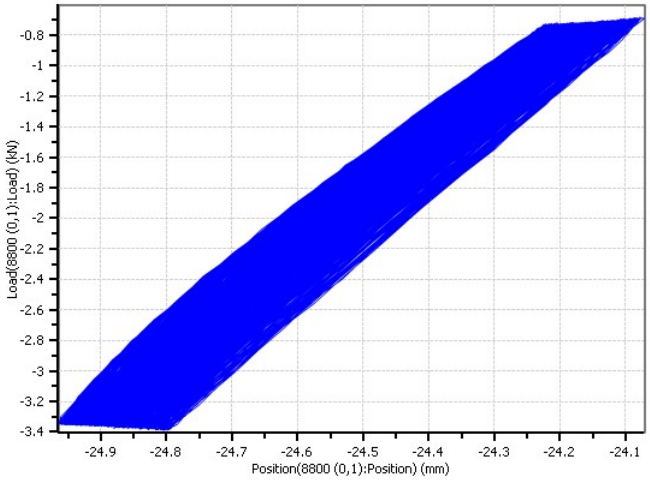


Figure III.15 Typical load-displacement graphic at the end of the test.

The graphic in the Fig. III.16 represented the proceeding of the dynamic test with 70% of mean load. As can be seen the minimum load on the graphic is 0.441 kN and the maximum load is 4.41 kN that corresponds to the table date of the P_{min} and P_{max} values.

The purpose of displacement-cycles graphics is controling the specimen displacement during the fatigue life. At the Fig. III.17 is the example of typical fatigue displacement-total cycles graphic is presented. Two parallel curves show the highest and the lowest points of piston movement in servo-hydraulic machine. The low piston position corresponds to the major displacement values, the first curve. This is due to the fact that in low position the piston unloads the specimen, while in high position it loads the specimen, the second curve. When the curves are parallels the specimen stiffness is constant. At the end of the fatigue test the graphic changes the geometry due to the failure occurrence.

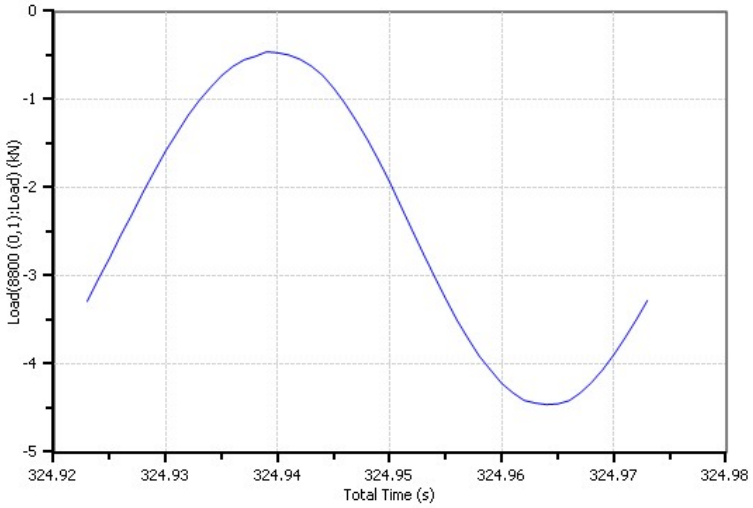


Figure III.16 Load-time graphic.

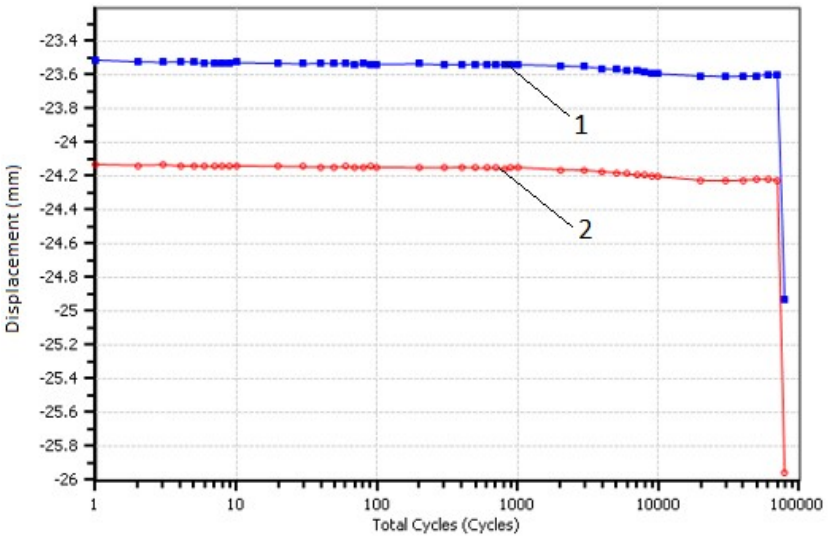


Figure III.17 Displacement-cycles graphic.

IV. Results and discussions

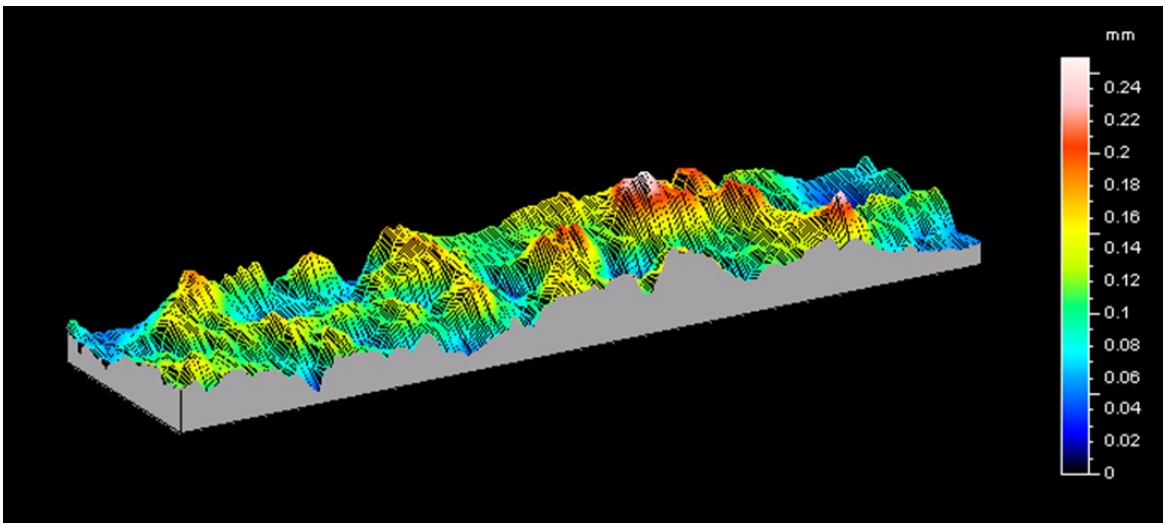
IV.1. Substrate mechanical treatment and roughness parameters.

In order to realize one of the principal objectives of present study, mechanically treated metallic plates were analyzed for roughness criterions before the bonding. The equipment used for roughness analyses was described in section IV.1. The values of the roughness parameters obtained throughout mechanical treatment are presented in table IV.1.

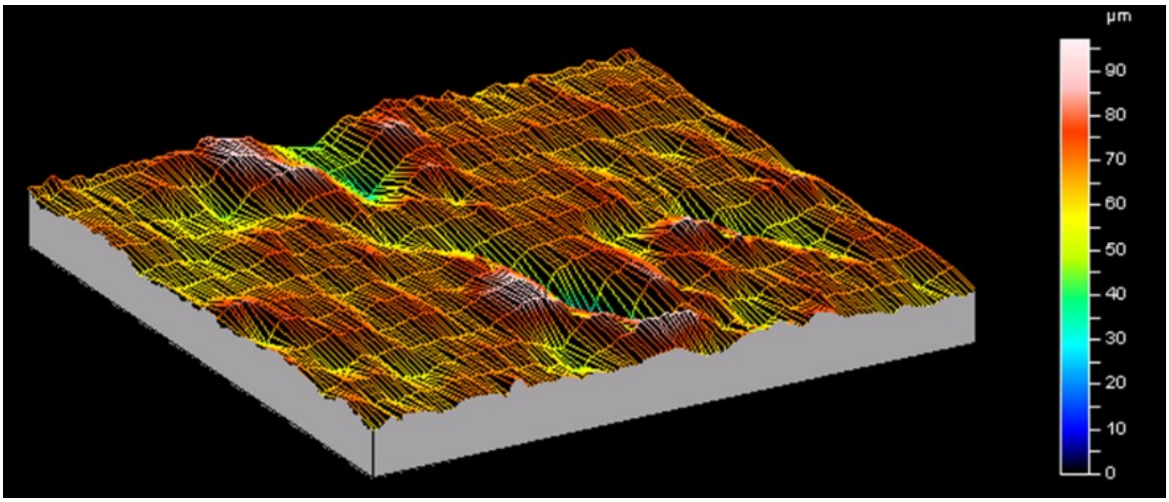
Table IV.1 Surface roughness parameters.

Treatment / Superficial parameter	**Symbol identification**	**Ra (µm)**	**Rt (µm)**
Grit blasting (G25)	R_{GB}	12.20	112.50
Sand blasting	R_{SB}	4.90	30.00
Bristle blasting	R_{BB}	4.66	45.15

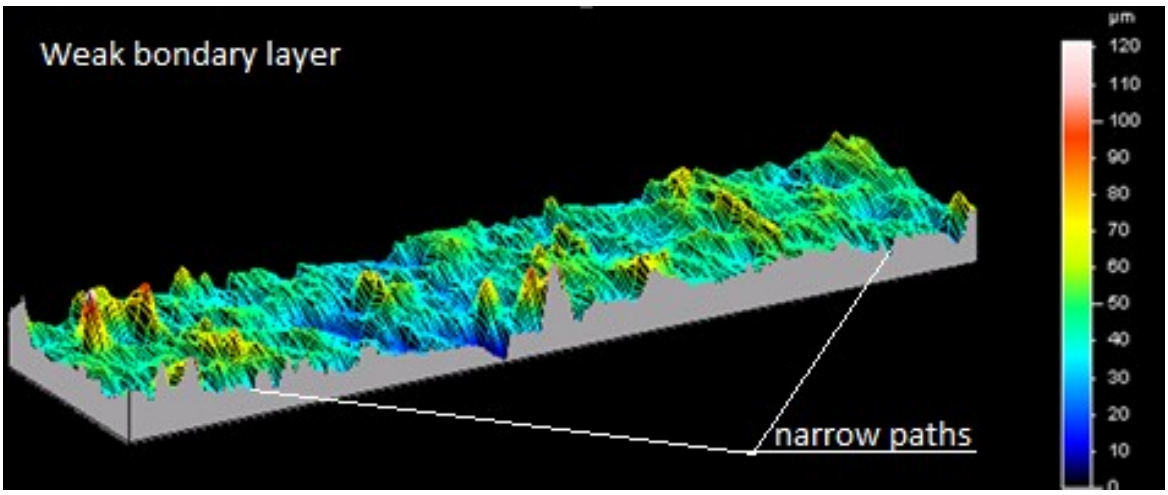
The mechanical treatment of metallic plates was realized in two different ways namely erosive and abrasive wear surface preparation. Erosive wear includes grit and sand blasting, abrasive wear includes bristle blasting treatment. Analyzing the roughness parameters of three mechanical treatment, made on substrates, it can be seen that bristle blasting mechanical treatment gives relatively low roughness and unevenness surface, comparing with the grit or sand blasting. Bristle blasting makes a surface as rough as sand blasting, i.e. $R_{a(BB)} \approx R_{a(SB)}$ but more unevenness in terms of picks and valleys, i.e. $R_{t(BB)} > R_{t(SB)}$. Grit blasting provides approximately three times rougher and uneven surface than sand blasting or bristle blasting. Generally, in terms of roughness level sand blasting and bristle blasting are similar. Figure IV.1 presents the images of surface profiles obtained with 3D surface roughness tester, mentioned previously. As can be seen from the image IV.1c bristle blasting surface contents narrow paths. This paths prevents the adhesive fills well all the valleys of the surface which results the presence of entrapped air in the paths which create the stress concentration points. This phenomenon is known as weak boundary layer. The weak boundary layer has negative effect on bonded joint quality and reduce its service life (section II.4). This analysis leads to conclusion that abrasive wear preparation provides a worse quality surface.



a)



b)



c)

Figure IV.1 Surface profiles after mechanical treatment:
a) grit blasted surface profile; b) sand blasted surface profile; c) bristle blasted surface profile.

IV.2. Thick adherent shear testing in monotonic regime.

Thick adherent shear test was realized with the objective to investigate how the bonded joints with different substrate mechanical treatment resist to shear stress in monotonic regime. Nine specimens with three types of mechanical treatment were tested. After the testing the obtained results is presented in Fig. IV.2.

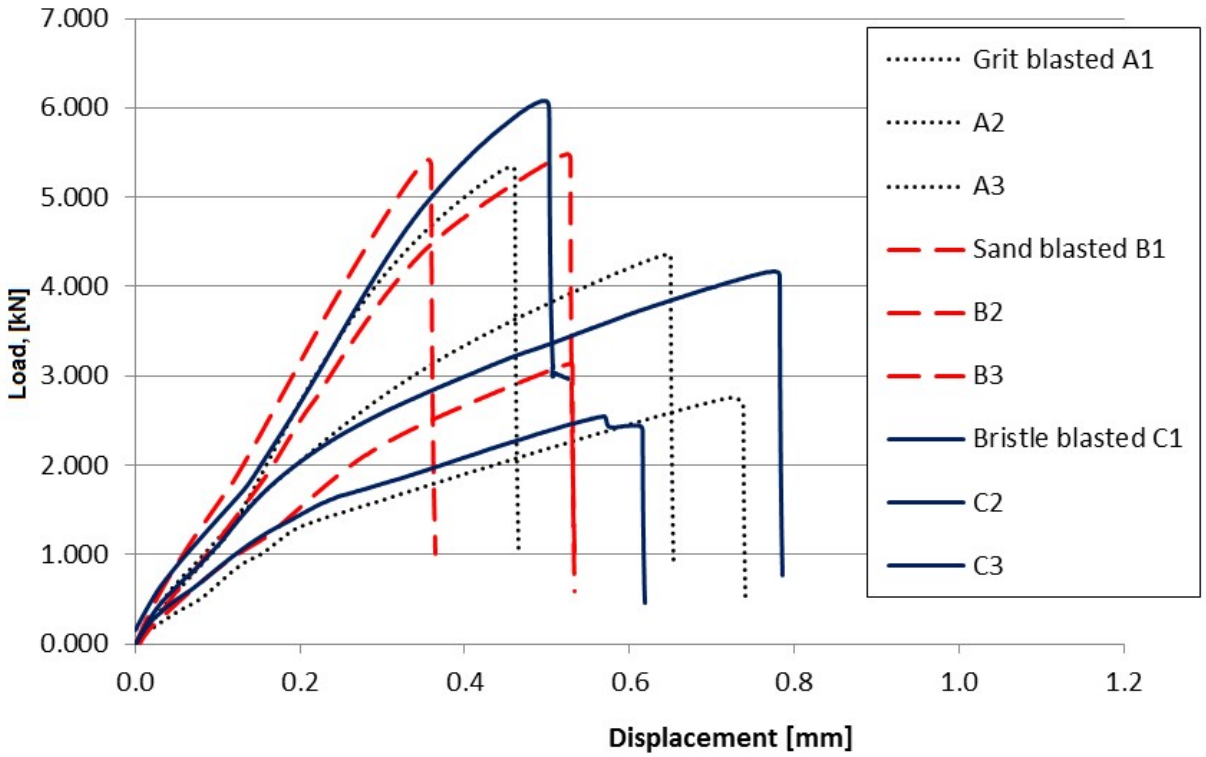
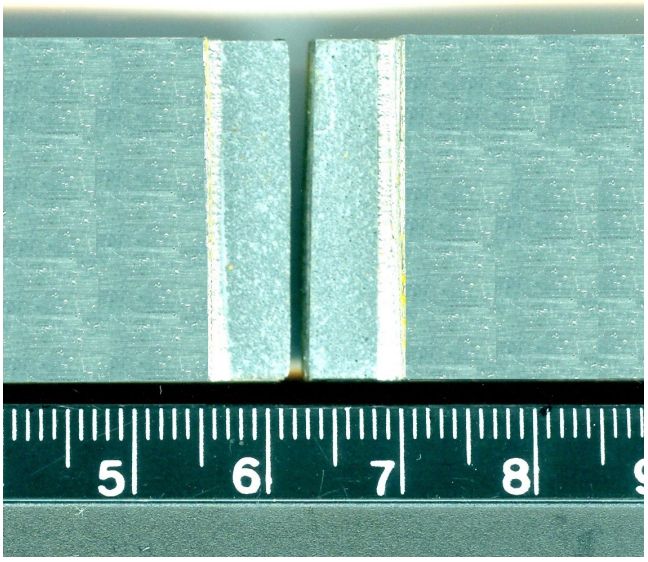


Figure IV.2 TAST results obtained for all the specimens.

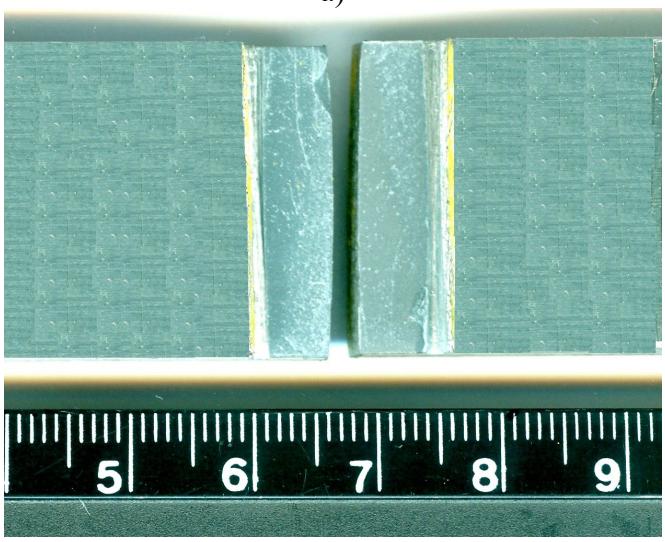
The specimens with three types of substrate mechanical treatment have shown the maximum strength in the range of 5,300-6,100 kN. In particular, bristle blasted specimens has showed the best resistance, sand blasted specimens has showed an intermediate result, and the worse one was of the grit blasted mechanical treatment. The obtained from the test curves have some dispersion. This is due to the fact that bonded area is very small which results in sensitivity of the test.

Additionally, shear stress of the adhesive was determined, τ = 48 MPa, based on the bristle blasting result.

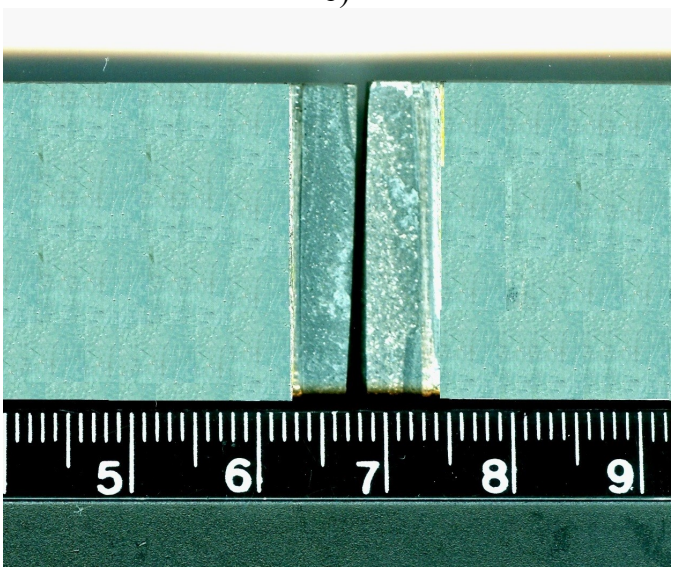
The quality of failure interface was found cohesive for all the types of surface mechanical treatment, as shown at Fig. IV.3.



a)



b)



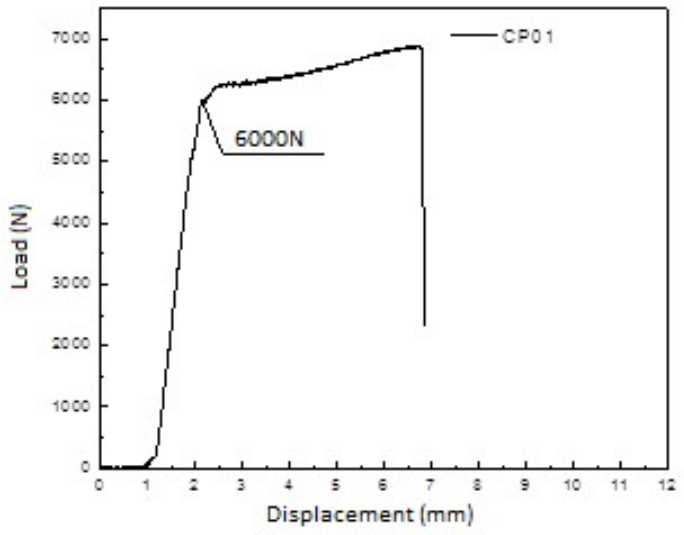
c)

Figure IV.3 Failure interface of the specimens after thick adherent shear testing: a) grit blasted specimen, b) sand blasted specimen, c) bristle blasted specimen.

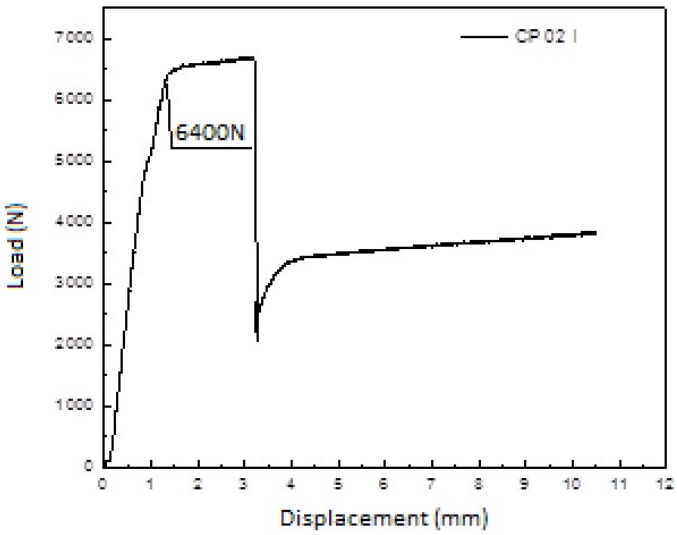
IV.3. Monotonic end-notched flexure testing.

End-notched flexure test is the most appropriate test format when bonded joints need to be submitted to shear loading. In this work monotonic ENF test was performed in order to examine the behavior of bonded joints and determine yield strength. The determined value was used for calculation of dynamic test parameters.

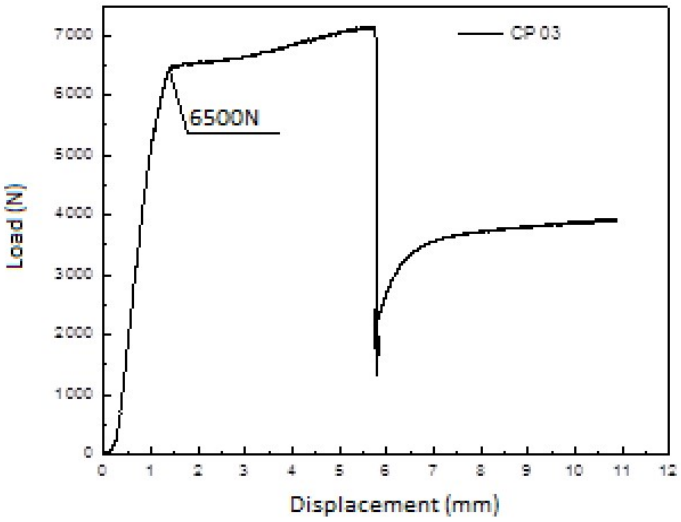
The test execution started with sand blasted specimens. Three sand blasted specimens were tested in monotonic regime and presented similar behavior during the tests. The load-displacement curves experimentally obtained are presented at Fig. V.4



a)



b)



c)

Figure IV.4 Load-displacement curve for static test of sand blasting specimens:
a) SP1 P_y = 6,000N; b) SP2 P_y = 6,400N; c) SP3 P_y = 6,500N.

Analyzing the load-displacement curve it is possible to see that the failure occurs after a significant plastic deformation of the specimen. The values of substrate yield strength were used to determine the maximum load of dynamic test program. The average yield point was calculated as $P_{(y)a}$ = 6,300N. Figure IV.5 shows a specimen after the testing.

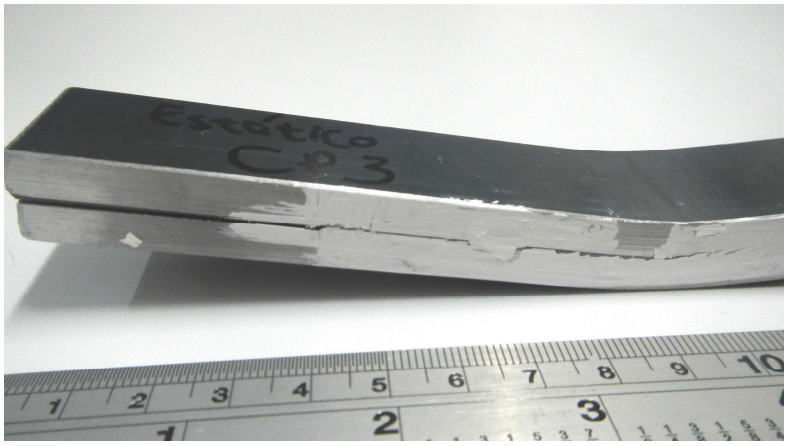


Figure IV.5 Grit blasted specimen after the testing in monotonic regime.

Bristle blasting and grit blasting specimens tested in static regime changed the geometry up to ultimate substrate material yielding. The failure didn't occur, therefore these tests weren't considered.

IV.4. Dynamic end-notched flexure testing

According to the average substrate yield strength calculated before, the fatigue test program was determined, as shown at Tab. IV.2.

Table IV.2 The fatigue test program.

Load level, f(%)	P_{max} (kN)	P_{min} (kN)	P_{amp} (kN)	P_{avr} (kN)	R
50	3.15	0.315	1.416	1.731	0.10
60	3.78	0.378	1.699	2.077	0.10
70	4.41	0.441	1.982	2.423	0.10
80	5.03	0.503	2.265	2.769	0.10

The quantitative results of fatigue tests are presented in Table IV.3 Dynamic tests performed at four different load levels showed significant influence of surface mechanical treatment on fatigue life of bonded joints.

Table IV.3 Results of fatigue test for the specimens with different mechanical treatment.

Load level, f(%)	P_{avr}, kN	P_{max} (kN)	P_{min} (kN)	Mechanical treatment/number of cycles, N		
				Grit blasting	Sand blasting	Bristle blasting
50	1.731	3.15	0.315	$1.1x10^6$	$1.2x10^6$	$3.7\ x10^4$
60	2.077	3.78	0.378	$2.9x10^5$	$7.2x10^5$	$2.7\ x10^4$
70	2.423	4.41	0.441	$2.2x10^4$	$2.4x10^4$	$4.8x10^3$
80	2.769	5.03	0.503	$2.9x10^3$	$1.8\ x10^4$	$3.7x10^3$

The load-cycles curves obtained from the fatigue tests are presented at Fig. IV.6. As can be seen, the fatigue tests results revealed a clear difference in the fatigue life for specimens with different mechanical treatment. Although all the tested specimens had a reasonable fatigue behavior, unexpectedly the joints that had the worse result in monotonic tests had the better results in fatigue tests.

The best performance in fatigue tests were obtained by the specimens that have been submitted to sand and grit blasting mechanical treatment, they overpassed 10^6 cycles. The specimens with bristle blasting treated substrates showed the worst results with maximum fatigue life of 10^4 cycles, which is two orders lower than the results of sand and grit blasted specimens. All these facts evidence the direct influence of mechanical substrate surface treatment to fatigue behavior of bonded joints.

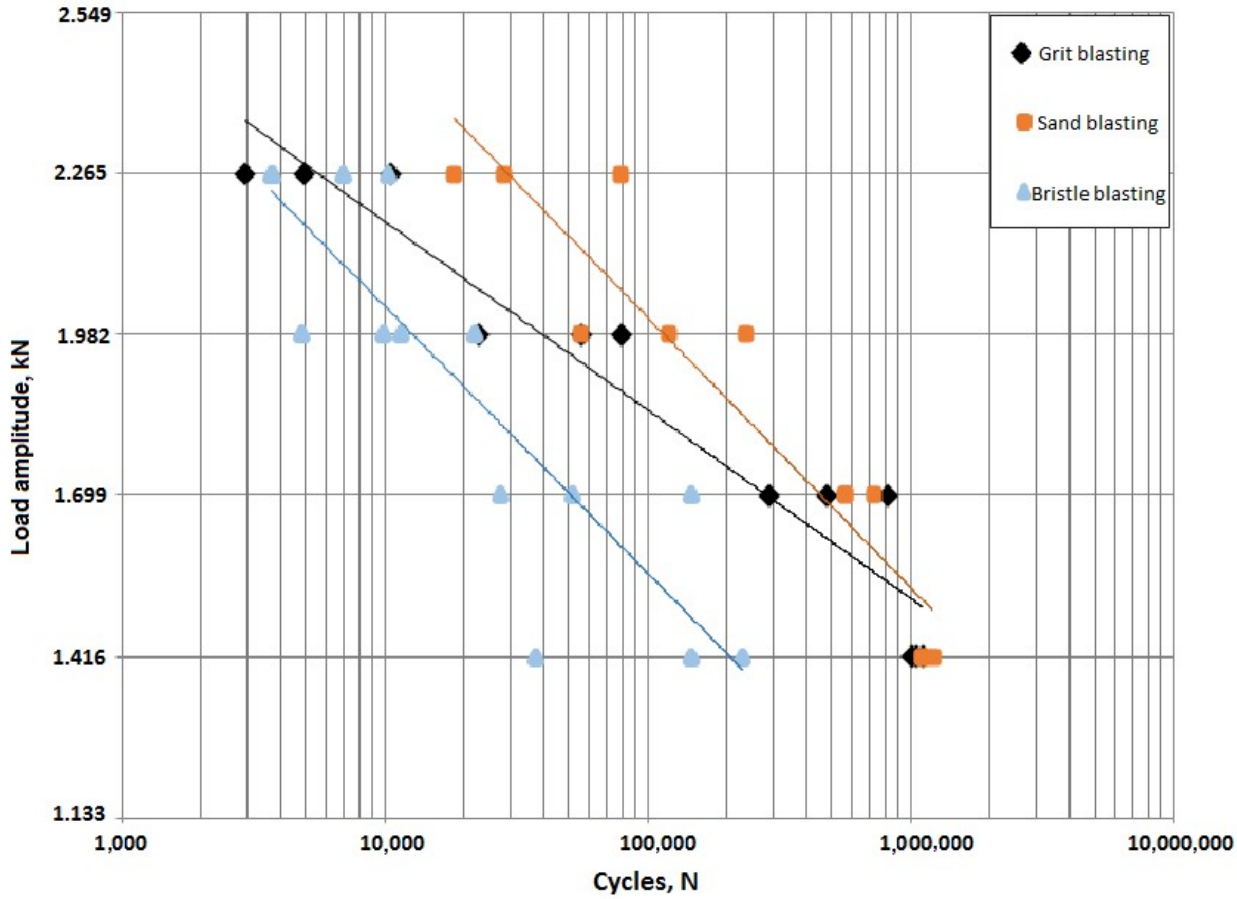


Figure IV.6 Load-cycles curves obtained for three types of substrate mechanical treatment.

IV.5. Failure locus analysis

After fatigue testing the specimens were opened manually for failure analysis. The failure interface had four different areas. In order to identify each area the load-displacement graphics of the final phase of the dynamic test were observed. One of these graphics is shown at Fig. IV.7. The graphic is divided in two parts: the part that is contoured between 23.7 - 24.4 mm, (more dense part) corresponds to fatigue life of the specimen, the other part of the graphic is the rest of the cycles that passed before the dynamic test was stopped. The vertical line between the two parts of the graphic evidences about a sudden failure. The difference in inclination of two parts of graphic indicates the difference of the stiffness of the specimen. In the end of the dynamic test the specimen de-bonds and looses the stiffness. Then the testing was finished. These considerations explain the identification of the areas on the failure interface that will be described next.

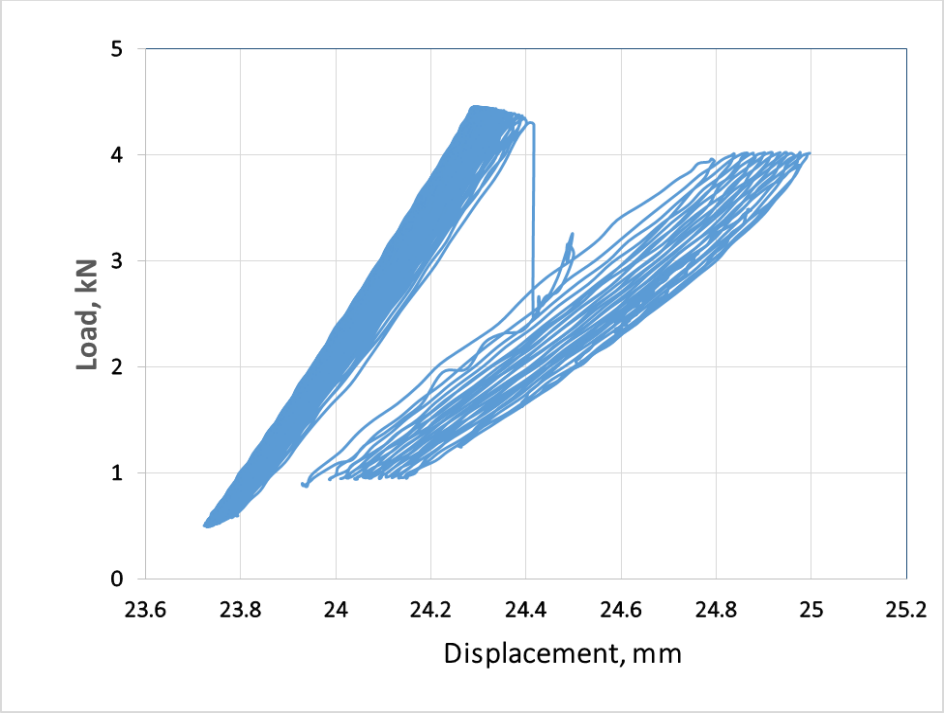
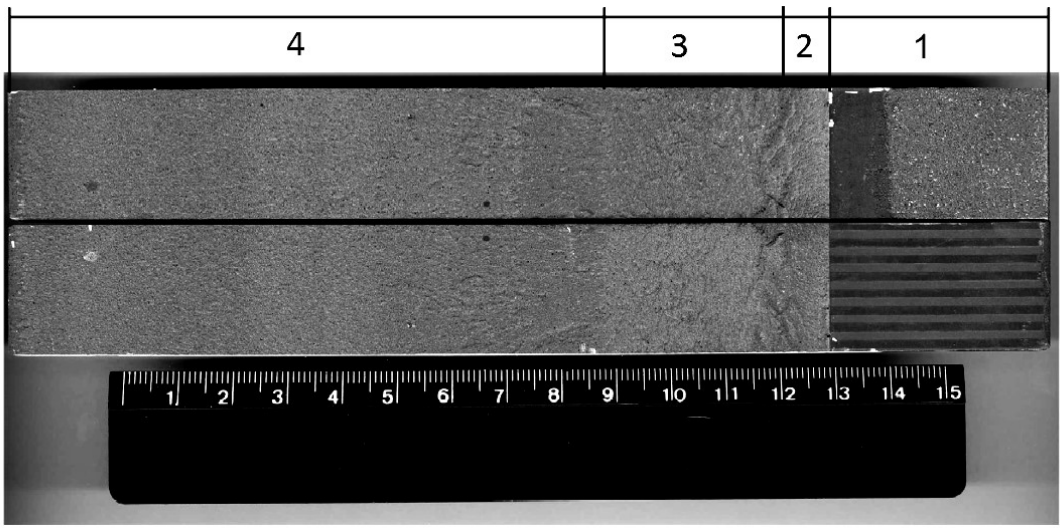
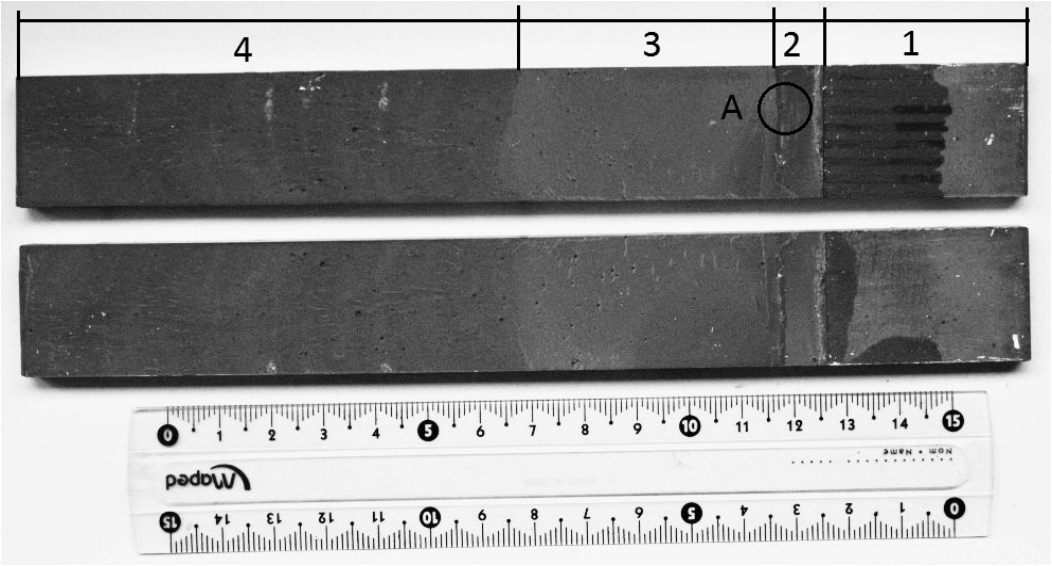


Figure IV.7 Load-displacement curve at the final phase of the fatigue test of the specimen M7T1(B).

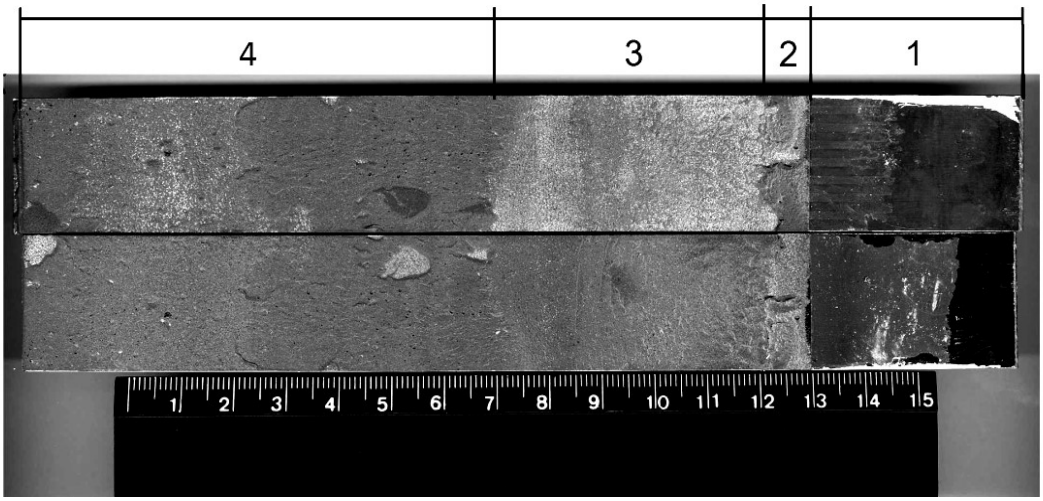
As can be seen at Fig. IV.8 each tested specimen has four numbered areas: the first area is the not bonded area. This area was leaved without bonding purposely in order to create a stress concentration line; the second area which has approximately 10 mm of length for all the specimens is necessarily fatigue failure locus that was formed during the cyclic loading until the failure occurred. The third area was formed as a result of specimen deboning that occurred in the last cycle of dynamic test. Between the second and the third area an inclined step was formed, with an inclined line of approximately 45° at lateral view as shown at Figs. IV.9 and IV.10.



a)



b)



c)

Figure IV.8 Failure interfaces of tested specimens: a) grit blasted failure interface, b) sand blasted failure interface, c) bristle blasted failure interface.

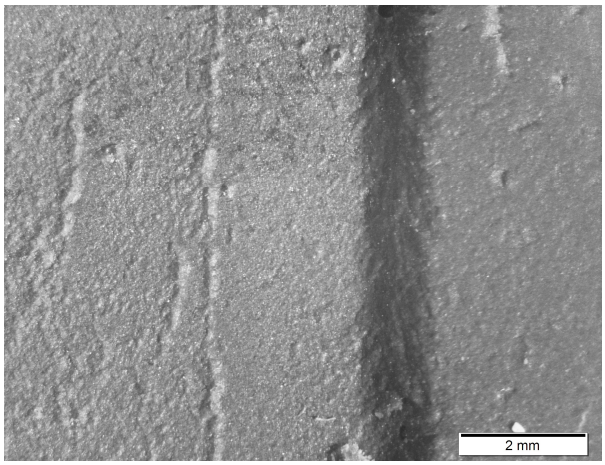


Figure IV.9 Top view of fragile failure line of the sand blasted specimen (A).

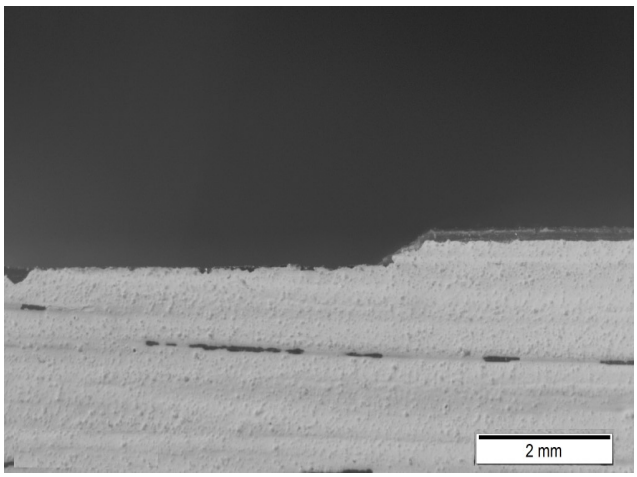


Figure IV.10 The Inclination of the fragile failure line (lateral view).

This line is typical fragile fracture line. The forth area is a result of manual opening of the specimen and is not considered in present study.

The failure locus of the tested specimens was also observed. It was detected, that grit blasted (Fig. IV.10, a) specimens and sand blasted (Fig. IV.10, b) specimens presented cohesive failure, while bristle blasted specimens presented mixed adhesive-cohesive failure under cyclic loading regime (Fig. IV.10, c). The difference in the interface failure quality is due to the different substrate mechanical treatment. From the theory that the quality of failure locus has direct correlation with substrate quality it can be concluded that bristle blasting treatment provides insufficient quality. Grit blasting and sand blasting are similar mechanical treatments that represent erosive wear while bristle blasting is abrasive wear of surface preparation. The insufficient quality of the abrasive wear surface preparation can be explained by the existence of a weak boundary layer. Detailed explication is in the chapter IV.1.

IV.6. Load analysis

The load level analysis was realized with the purpose of investigation of the influence of load level on the failure of bonded joints under cyclic loading. For this load-displacement curves of the final phase of fatigue test of different load levels were considered. It was observed that specimens with different mechanical treatment had similar behavior under the same level of load level. Therefore, load-displacement curves of sand blasted specimens with three different levels of loading were examined. In next figures IV.11, IV.12, IV.13, IV.14 are presented load-displacement curves of sand blasted specimens tested under 50% 60%, 70%, 80% of load level. As can be seen from the graphics, the specimens tested under three different load levels after the failure occurred there were some loss of stiffness. This is evidenced by the difference in angle inclination on the graphics. The specimen tested under 60% of load level loses stiffness at relatively slow rate. The specimens tested under with 70% and 80% of mean load lose the stiffness in a more sudden transient. The applied load diminishes also significantly.

The conclusion of the load analysis is can be described as follow: the heavier level loading induces more sudden manner of failure and loss of the joint stiffness.

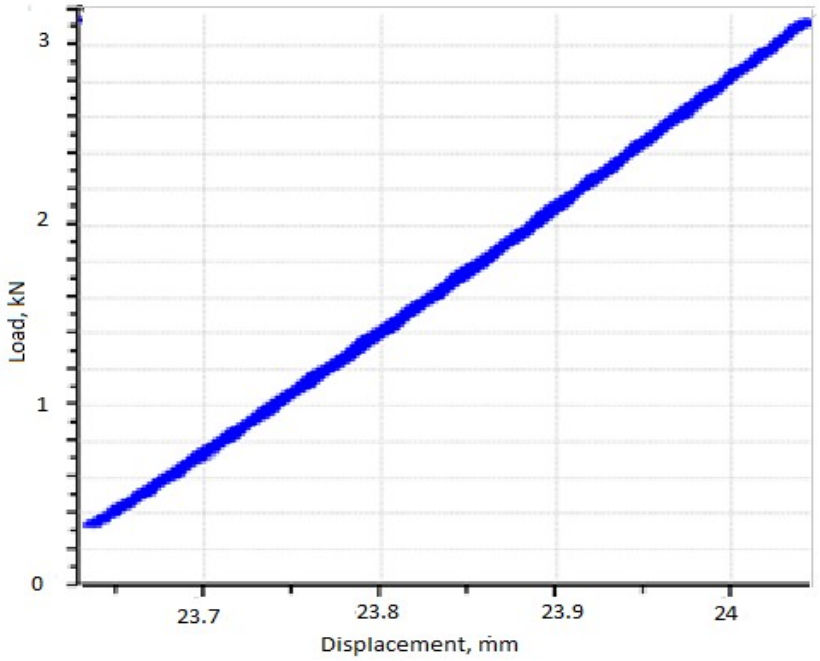


Figure IV.11 Load-displacement curve at the final phase of the fatigue test of the sand blasted specimen tested under 50% of load level.

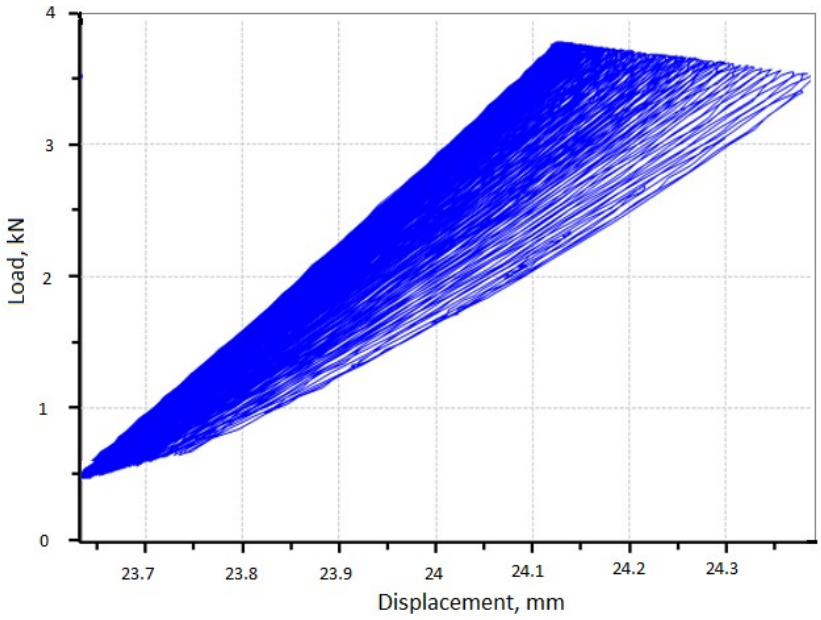


Figure IV.12 Load-displacement curve at the final phase of the fatigue test of the sand blasted specimen tested under 60% of load level.

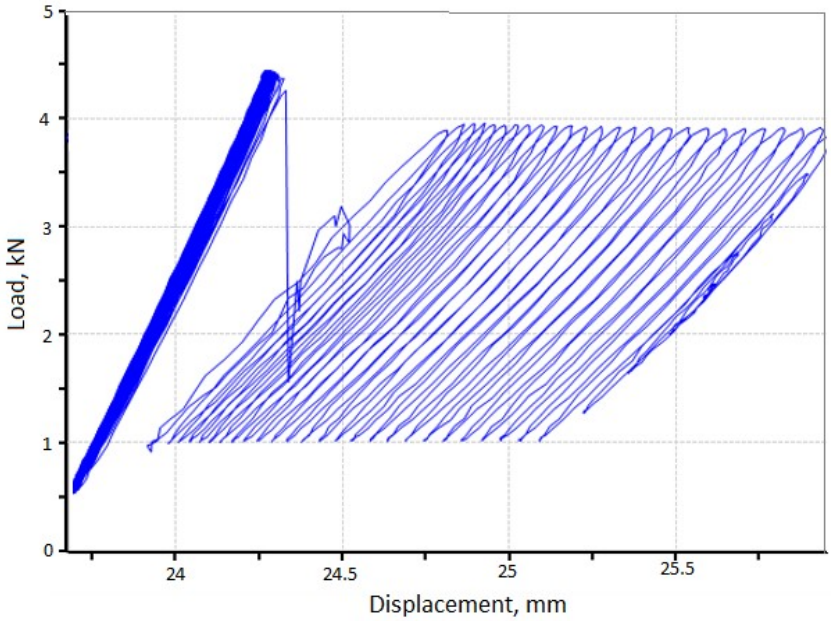


Figure IV.13 Load-displacement curve at the final phase of the fatigue test of the sand blasted specimen tested under 70% of load level.

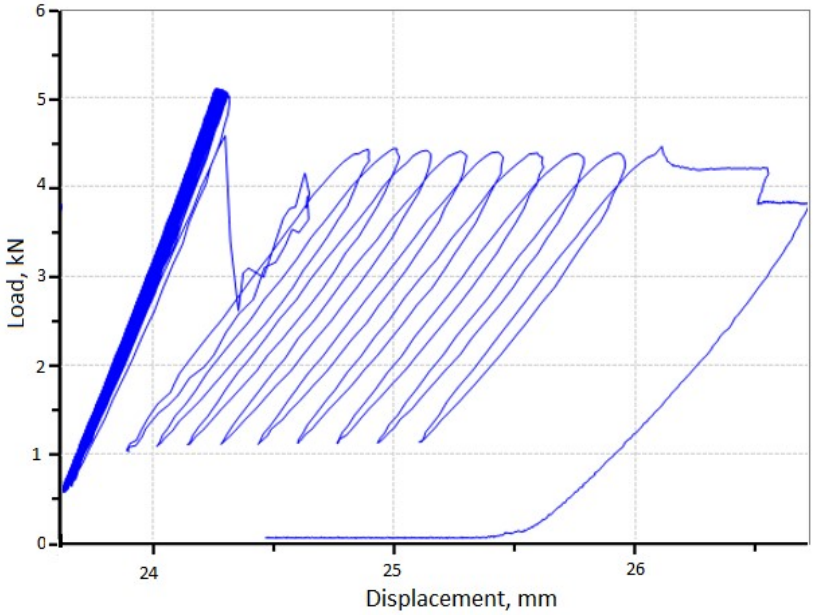


Figure IV.14 Load-displacement curve at the final phase of the fatigue test of the sand blasted specimen tested under 80% of load level.

IV.7. Crack length analyses

When the specimens have been dynamically tested, the loading was applied till the failure occurred. Resulting crack spreads through the second and third area in the failure locus (Fig. IV.8). Crack length analyses was realized with the purpose of determining the dependence between the load level and the final crack length in bonded joints. To accomplish this objective

cracks of all the tested specimens were measured and analyzed. The data base of the measured crack lengths is presented in table IV.4 As it can be seen from the table grit blasted and sand blasted specimens didn´t failure under 50% of load level.

Table IV.4 Crack length measurements.

Load level, %	Crack length, mm								
	Grit blasted specimens			Sand blasted specimens			Bristle blasted specimens		
	SP1	SP2	SP3	SP1	SP2	SP3	SP1	SP2	SP3
50	0	0	0	0	0	0	33	57	46
60	36	44	42	60	32	42	37	28	42
70	44	48	0	54	57	59	56	57	54
80	54	46	58	57	56	63	57	84	56

In order to facilitate the crack analysis average crack length sizes and relative crack length sizes were calculated and presented in table IV.5 Relative crack length size is determined as crack length related to the bonded length of the specimen.

Table IV.5. Calculated values of crack length sizes.

Load level, %	Bonded length, mm	Grit blasted specimens		Sand blasted specimens		Bristle blasted specimens	
		Average crack length, mm	Portion of bonded length, %	Average crack length, mm	Portion of bonded length, %	Average crack length, mm	Portion of bonded length, %
50	135	0	0	0	0	45	34
60	135	41	30	45	31	36	26
70	135	46	34	57	42	44	33
80	135	53	39	59	43	63	46

At Fig. IV.15 the diagram based on the calculated values of the average crack sizes and relative crack sizes is presented. Due to the fact that grit and sand blasted specimens did not de-bond under 50% of load level, the crack length analysis considered three load levels only, i.e. 60%, 70%, 80%. Crack length analysis showed that the final crack length increases as the load level increases for all the types of mechanical treatment.

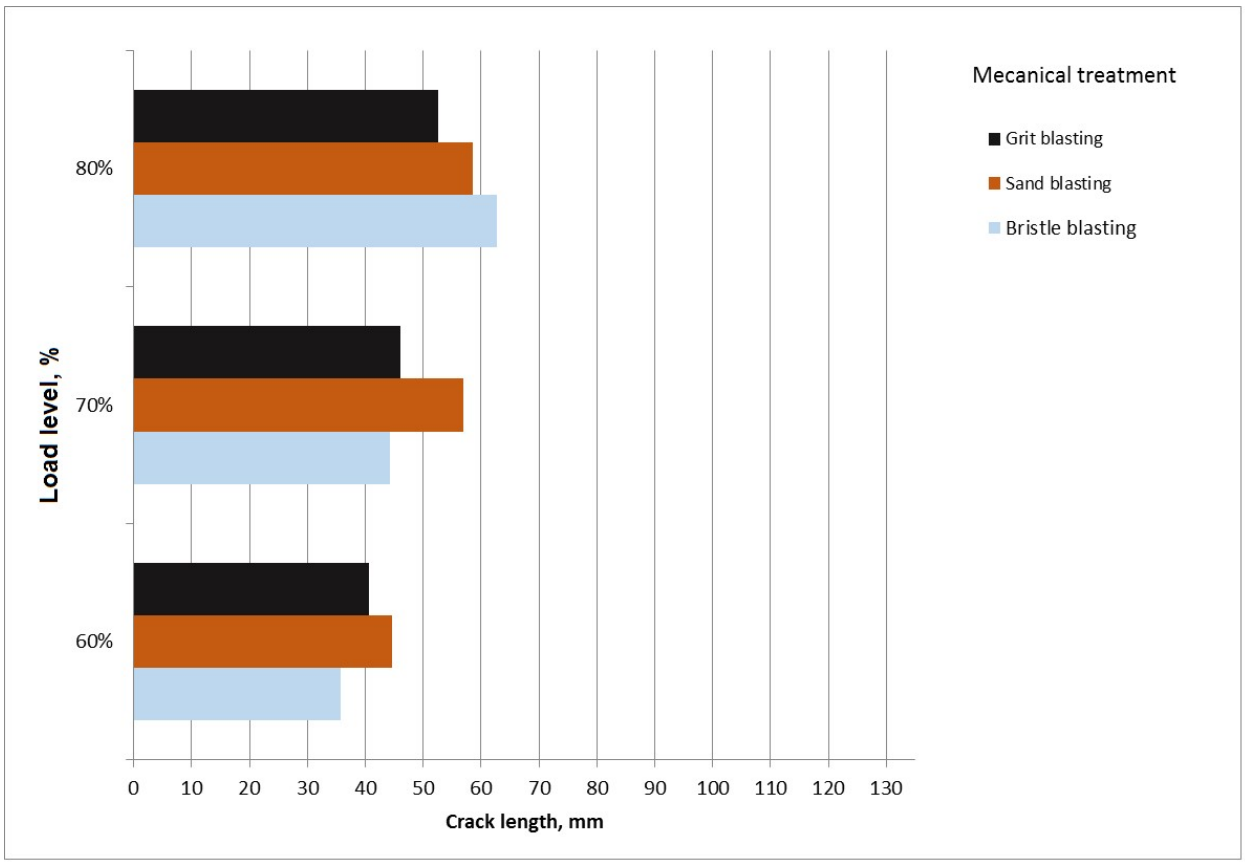


Figure IV.15 Crack length diagram.

IV.8. Crack propagation analyses

In order to investigate the crack behavior during the fatigue test, inside the second area of the failure locus (Fig. IV.10) the graphics load-displacement and displacement-cycles were analyzed. The purpose of displacement-cycles graphics is controlling the specimen displacement during the fatigue test. Two parallel curves shows the highest and the lowest points of the piston vertical movement in testing machine which ultimately represents the spacemen midpoint vertical displacement.

Detailed behavior of specimens with each treatment is described next. The load-displacement graphic represents the initial phase of the dynamic test of the sand blasted specimen, performed under load level 6 is shown at Fig. IV.15. In this initial phase of testing, after some loading cycles the certain level of specimen displacement was established that corresponds to -24.35 mm in the highest point and to -23.87 mm in the lowest one. The difference between these two values was 0.47 mm. As it can be observed, the values of the displacements -24.35 mm and -23.87 mm on the displacement-cycles graphic (Fig. IV.19) correspond to 10 cycles of the fatigue test.

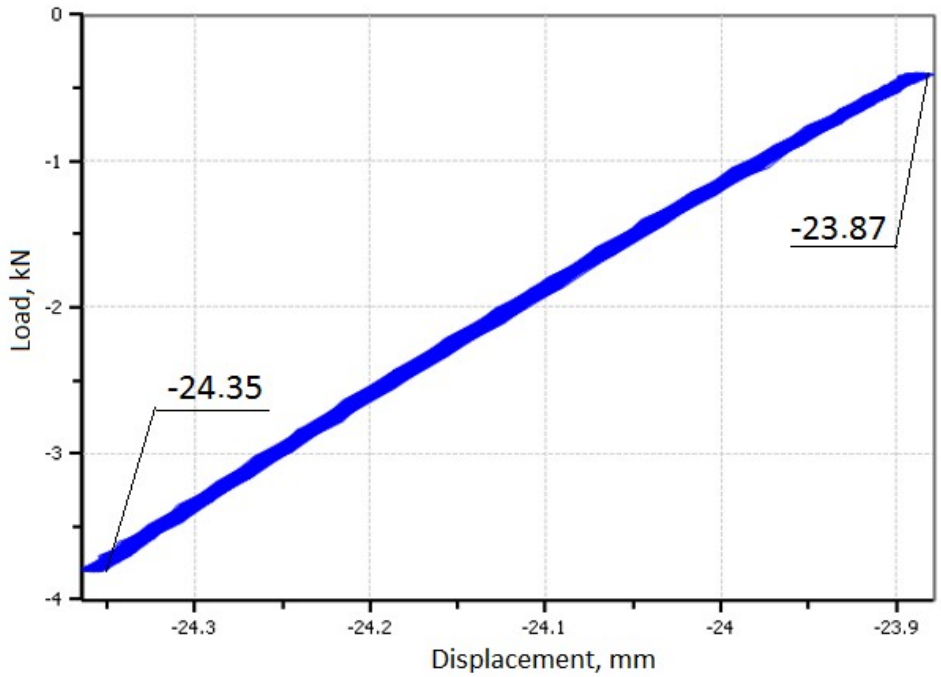


Figure IV.16 Load-displacement curve in the initial phase of the fatigue test of the specimen M6T1(B).

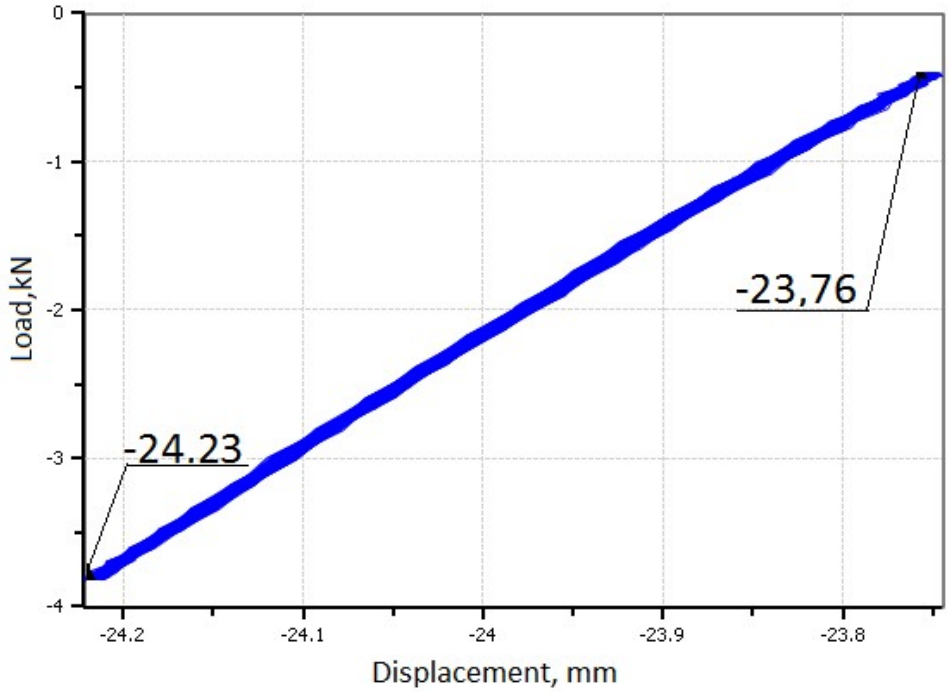


Figure IV.17 Load-displacement curve at 252,342 cycles of the fatigue life of the specimen M6T1(B).

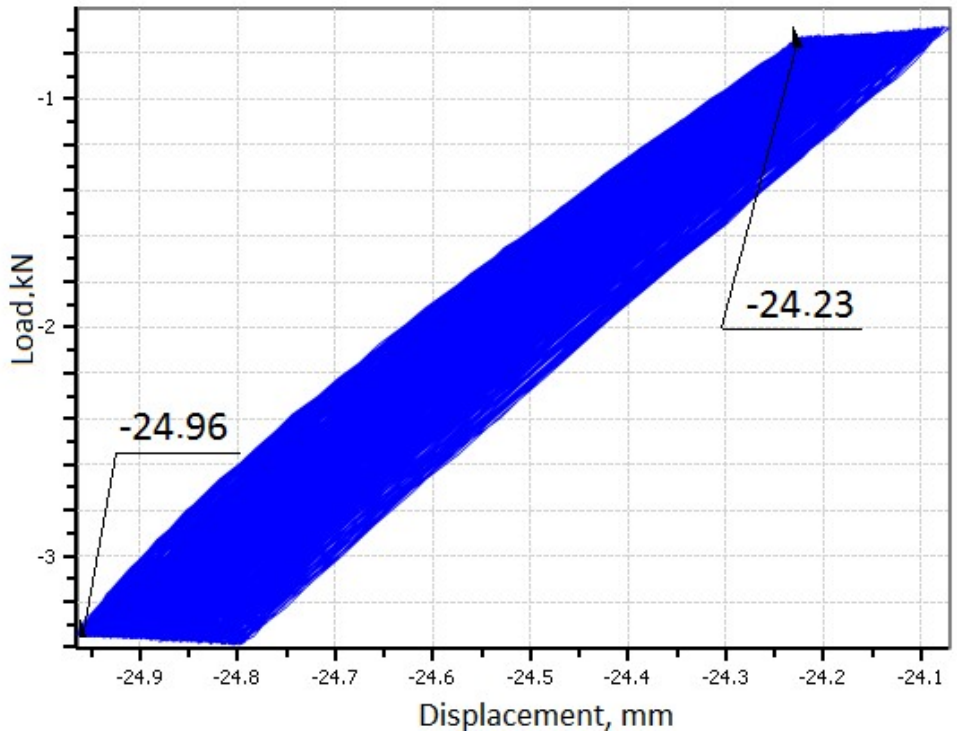


Figure IV.18 Load-displacement curve at the final phase of the fatigue test (565,249 cycles) of the specimen M6T1(B).

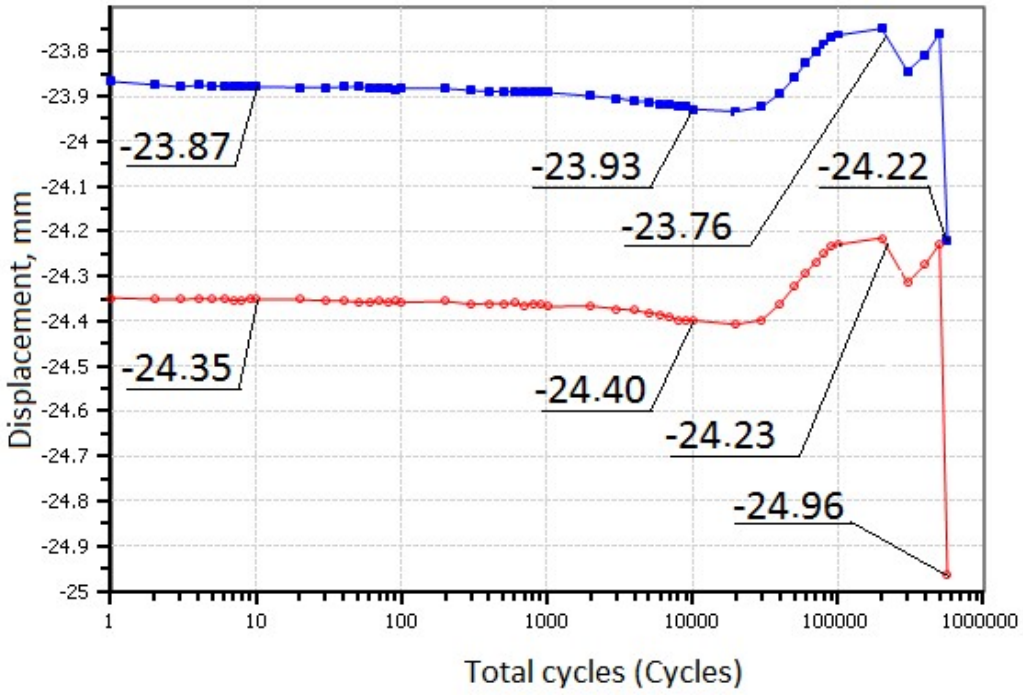


Figure IV.19 Displacement-Total cycles curve registered the fatigue life of 565,249 cycles of the specimen M6T1(B).

After some hours of testing proceeding and 252,342 cycles passed to that moment the testing was stopped. The load-displacement curve was registered again (see Fig. IV.17). It is seen that the difference between the highest and the lowest displacement points, i.e. -24.23 mm and 23.76 mm respectively, result in 0.48 mm. On the displacement-cycles curve the corresponding point is localized between 10^5 and 10^6 cycles. Then the testing was continued till

the failure occurred. The total fatigue life of M6T1(B) specimen was 565,249 cycles. At the moment of failure occurrence the load-displacement curve showed the major displacement, i.e. -24.96 mm and -24.23 mm, which results in 0.73 mm of specimen displacement, Fig. IV.18. This is clear evidence that the specimen lost stiffness.

On the Fig. IV.20, IV.21 are presented load-displacement and displacement-total cycles curves of the grit blasted specimen tested under the same conditions as a sand blasted specimen. The specimen M6T1(A) had 289,398 cycles of fatigue life. The testing was conducted without stopping. The load-displacement curve in the final phase of fatigue test is similar to the load-displacement curve of previous specimen. At some moment the inclination angle of the curve changes, and this means that the stiffness of the specimen changes, i.e. failure occurs. From displacement-cycles curve it is seen that the specimen displacement varies from 0.45 to 0.47 mm during the fatigue test, then at the last cycles it became 0.58 mm that evidences about failure.

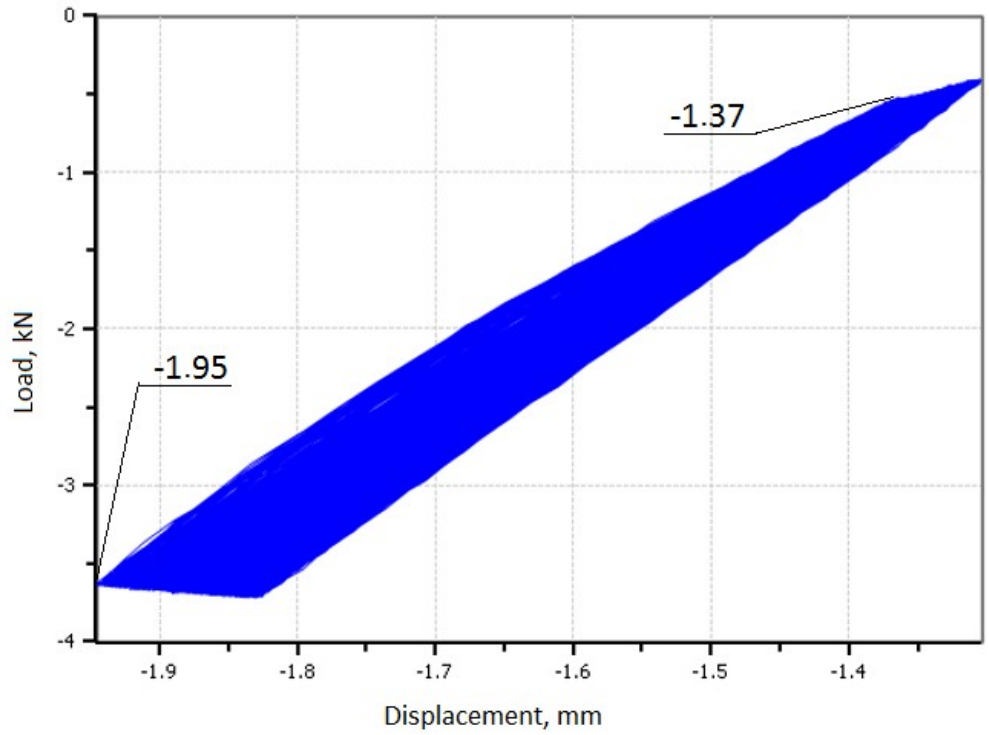


Figure IV.20 Load-displacement curve at the final phase of the fatigue life (289,398 cycles) of the specimen M6T1(A).

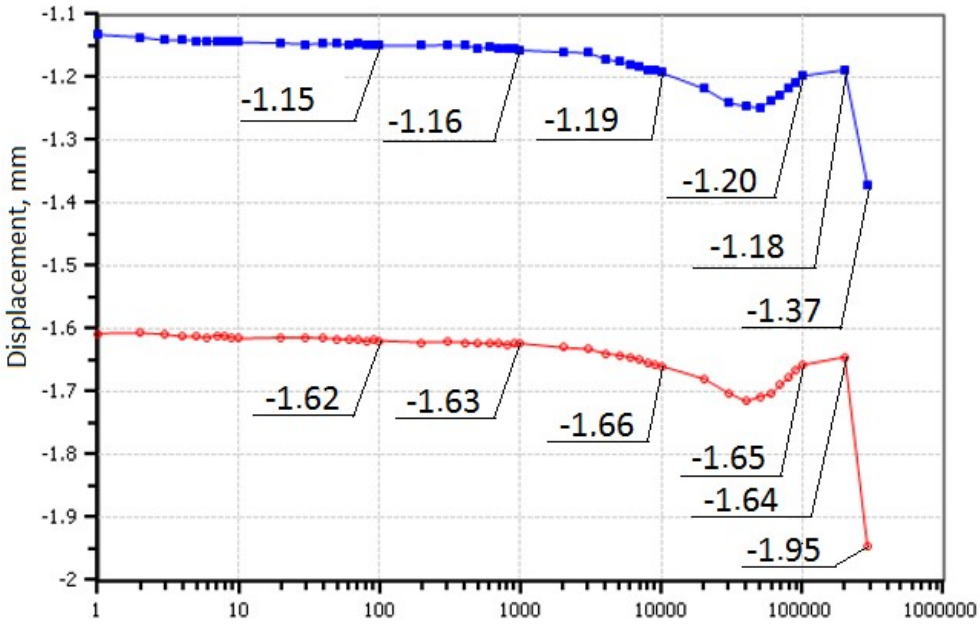


Figure IV.21 Displacement-Total cycles curve registered the fatigue life of 289,398 cycles of the specimen M6T1(A).

The behavior of bristle blasted specimens was similar to the sand blasted specimens. At Figs. IV.22, IV.23 there are the curves of load-displacement and displacement-total cycles of the specimen M6T2(C). Again, the displacement-total cycles curve showed the specimen displacement in range of 0.5 - 0.51 mm during the fatigue test, then after the failure the displacement became 0.60 mm.

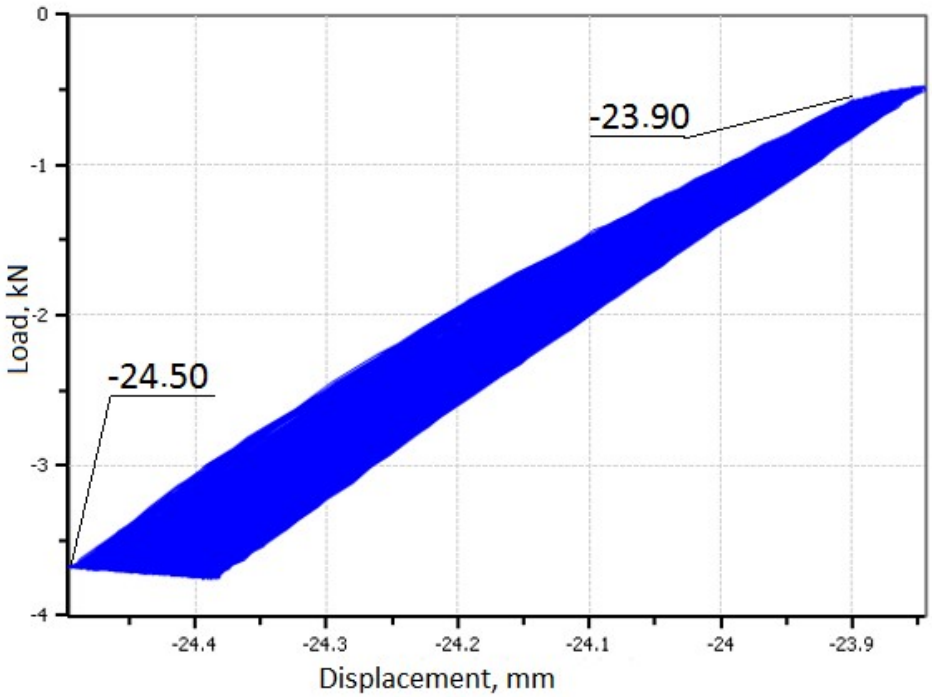


Figure IV.22 Load-displacement curve at the final phase of the fatigue life (52,040 cycles) of the specimen M6T2(C).

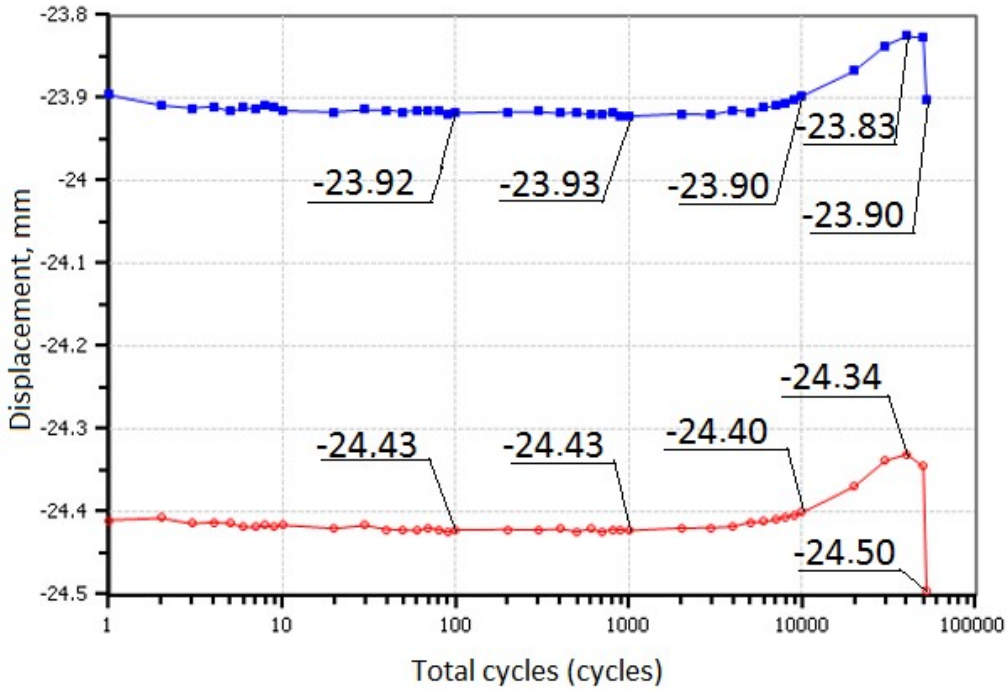


Figure IV.23 Displacement - Total cycles curve registered the fatigue life of 52,040 cycles of the specimen M6T2(C).

Three specimens with different mechanical treatment tested under 60% of mean load (Table IV.2) showed similar response to dynamic loading in the initial phase. The curves of five different specimens are shown at appendix. The specimen displacement oscillates in certain range for each specimen. Increase in the displacement range evidences about the failure. All the observations, obtained from the graphics allow to conclude that the specimens had constant stiffness during all the dynamic test. This conclusion leads to suppose about stable crack propagation inside the second area of failure locus (Fig. IV.8) However, it´s yet not possible to determine the threshold between the crack nucleation and the crack propagation phases.

V. Conclusions and suggestions

V.1. Conclusions

The main purpose of this work was to study the influence of mechanical treatment of substrate surface to high cycle fatigue resistance of adhesively bonded joints under shear mode. The important aspect of this research was to evaluate and compare the fatigue resistance of bonded joints with grit, sand and bristle blasting mechanical treatments. The tests were performed in end-notched flexure format in high-cycle fatigue regime. Thick adherent share test was also performed with the objective to compare the resistance of the joints in monotonic and dynamic regimes. The results obtained from experimental tests are presented. Surface roughness, failure locus, load level, crack length and crack propagation analysis were carried out. The influence of surface mechanical treatment of adhesively bonded joints was investigated.

The results from experimental investigation showed that substrate mechanical treatment that provides a certain roughness on a substrate plays a significant role in fatigue resistance of adhesive joints. Moreover, the joint durability is not only depends on the roughness level of the substrate itself but also the way the roughness is produced, that in turn, influences the quality of treated surface. Thus, grit blasted and sand blasted joints, that have erosive wear preparation, have fatigue life, overcoming 10^6 cycles. Bristle blasted joints, with abrasive wear preparation, lasted only 10^4 cycles under dynamic loading. Resistance to monotonic loading of the same kind of joints doesn't corresponds to their fatigue resistance. All the joints had maximum monotonic resistance of 5-6 kN. The influence of load level on the fatigue resistance of bonded joints was found significant and can be described as follow: as the mean load increases the resistance reduces and the failure can occur in a more sudden way. The relation between load level and crack length can be described as follow: when the load level increases the crack length increases for all kinds of joints.

Finally, fatigue testing results leads to conclusion that abrasive wear surface preparation provides insufficient surface quality that reduces significantly the joint service life. In terms of the failure interface quality grit blasted and sand blasted joints had cohesive failure, while bristle blasting treatment had adhesive failure.

V.2. Suggestions for future works

There is a lot of room for future research in this relatively new field. Particularly crack propagation analysis made in present study is based on the examination of displacement-total cycles curves captured in the final phase of fatigue test. This analysis provides qualitative result only. In order to obtain the quantitative result the whole data base should be considered.

Bristle blasting substrate treatment needs to be studied more detailed for influence the weak boundary layer on joint quality. Detailed investigation of the treated surface should be made before the bonding. This would confirm the result obtained in present work about insufficient quality of erosive wear surface preparation. The importance of this study is explained by the fact that bristle blasting treatment is widely used in industry nowadays.

References

ADAMS, R., D., WAKE, W. C.; *Structural Adhesive Joints in Engineering*, London, El sevier, 1986.

AZARI, S., PAPINI, M., SPELT, J.K., “Effect of surface roughness on the performance of adhesive joints under static and cyclic loading”, The Journal of Adhesion, v. 86, p.742-746, 2010.

ASTM D638-14, Standard Test Method for Tensile Properties of Plastics, ASTM International, West Conshohocken, PA (2014).

ASTM D2240-05(2010), Standard Test Method for Rubber Property—Durometer Hardness, ASTM International, West Conshohocken, PA (2010).

ASTM A36 / A36M-14, Standard Specification for Carbon Structural Steel, ASTM International, West Conshohocken, PA (2014).

ASTM D3165-07(2014), Standard Test Method for Strength Properties of Adhesives in Shear by Tension Loading of Single-Lap-Joint Laminated Assemblies, ASTM International, West Conshohocken, PA, 2014.

ASTM E739-91(1998), Standard Practice for Statistical Analysis of Linear or Linearized Stress-Life (S-N) and Strain-Life (e-N) Fatigue Data, ASTM International, West Conshohocken, PA, 1998.

BERMEJO, R., ONORO, J., GARCIA-LEDESMA, R., “Comportamiento a fatiga de uniones a solape com adesivo epóxi de acero y acero prepintado”, Revista de Metalurgia, v. 44, pp. 310-316, 2008.

BERNASCONI, A., BERETTA, S., MORONI, F., PIRONDI, A., et al., “Load stress analysis of fatigue behaviour of adhesively bonded thick composite laminates”, The Journal of Adhesion, v. 86, pp. 480-492, 2010.

BLAND, D. J., KINLOCH, A. J., WATTS, J. F.; “The role of the Surface Preatreatment in the Durability of Aluminium-Alloy Structural Adhesive Joints: Mecanisms of Failure”, The Journal of Adhesion, v. 89, n. 5, pp. 369-397, 2013.

CHANDER, K. P., VACHISTA, M., SABIRUDDIN, K., PAUL, S., BANDYOPADHYAY, P. P.; “Effect of grit blasting on surface properties of steel substrates”, Materials and Design, v. 30, pp. 2895-2902, 2009.

DA FONSECA, A. H. M; “Proposta de um critério de resistência para juntas metálicas coladas”, Dissertação de Mestrado, UFF, Rio de Janeiro, RJ, Brasil, Setembro de 2007.

DA SILVA, L. F. M; MAGALHÃES, A. G.; MOURA, M. F. S. F.; Juntas adesivas estruturais, Porto, Publinduistria, 2007.

DA SILVA, L.F.M., CARBAS, R. J. C., CRITCHLOW, G. W., FIGUEIREDO, M. A. V., BROWN, K.; “Effect of material, geometry, surface treatment and environment on the shear

strength of single lap joints", International Journal of Adhesion&Adhesives, v. 29, pp. 621-632, 2009.

DE BARROS, S., DE SOUZA, J. R., GOMES, K.C., SAMPAIO, E. M., BARBOSA, N. P., TORRES, S. M.; "Adhesion of the geopolymer bonded joints considering surface treatments", The Journal of Adhesion, v. 88, pp. 364-375, 2012.

HARRIS, A.F., BEEVERS, A., "The effect of grit-blasting on surface properties for adhesion"; International Journal of Adhesion&Adhesives, v. 19, pp. 445-452, 1999.

ISO 4288-1996. Geometrical Product Specifications (GPS) - Surface texture: Profile method - Rules and procedures for the assessment of surface texture.

ISO 11003:2 2001 Adhesives - Determination of shear behaviour of structural adhesives - Part 2: Tensile test method using thick adherends.

KUCZMASZEWSKI, J., Fundamentals of metal-metal adhesive joint design, Lublin, Polish Academy of Sciences, 2006.

MENICONI, L. C. M, LANA, L. D. M., MORIKAWA, S. R. K., "Experimental fatigue and evaluation of the composite patch of a metallic ship hull", A Springer Open Journal of Applied Adhesion Science, pp. 2-27, 2014.

MULLER, M.; "Influence of surface integrity on bonding process"; Research in Agricultural Engineering, v. 57, pp. 153-162, 2011.

SAHOO, P.K., DATTAGURU, B., MANJUNATHA, C. M., MURTHY, C. R. L.; "Fatigue de-bond growth in adhesively bonded single lap joints", Indian Academy of Sciences, v. 37, n. 1, pp. 79-89, 2012.

THEVENET, D., CREAC´HCADEC, R., SOHIER, L., COGNARD, J. Y.; "Experimental analysis of the behavior of the adhesively bonded joints under tensile/compression-shear cyclic loadings", International Journal of Adhesion&Adhesives, v. 44, pp. 15-25, 2013.

WU, S.; Polymer interface and adhesion, New York, 1982.

Journal of Pharmacy. Bio Allied Science. Available in: < http://www.jpbsonline.org/article.asp?issn=0975-7406;year=2011;volume=3;issue=1;spage=89;epage=100;aulast=Shaikh> Accessed in 8th of July 2015.

Teach engineering. Lesson: Wetting and contact Angle. Available in: < https://www.teachengineering.org/view_lesson.php?url=collection/duk_/lessons/duk_surfacetensionunit_lessons/duk_surfacetensionunit_less3.xml> Accessed in 8th of July 2015.

Adhesives. Available in: < http://www.adhesives.org/adhesives-sealants/science-of-adhesion/adhesion-cohesion> Accessed in 20th of August 2015.

Azo Materials. Fatigue Testing System – Model 8801 from Instron. Available in: < http://www.azom.com/equipment-details.aspx?EquipID=1183> Accessed in 15th of March 2015.

Archiproducts. IBIX 25. Available in: < http://www.archiproducts.com/pt/produtos/11237/decapagem-limpeza-por-jacto-de-areia-esmerilamento-ibix-25-ibix.html > Accessed in 15th of March 2015.

Consumables Express Ltd. MBX air-op machine. Available in: < http://www.consumablesexpress.co.uk/mbx-air-op-machine-c-w-3-belts-> Accessed in 8th of July 2015.

Bestar Group Co., Limited. Available in: < http://sinobestar.sell.everychina.com/p-102514565-cast-steel-grit-g80-0-3mm.html> Accessed in 13th of March 2015.

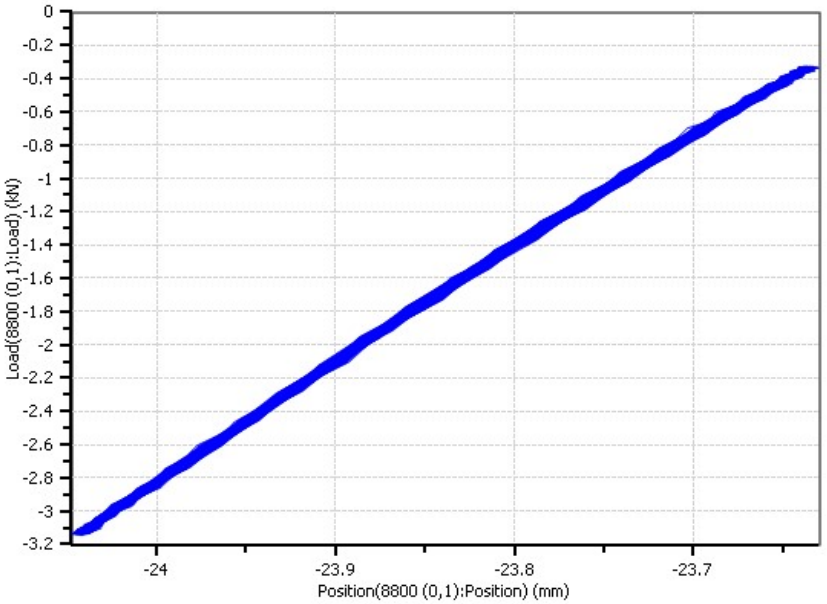
Diy Trade. Global B2B Trading Paltform. Garnet abrasive sand-blasting metal. Available in: < http://www.diytrade.com/china/pd/12067401/Garnet_abrasive_sand_blasting_metal.html> Accessed in 13th of March 2015.

Taylor Hobson. 3D Image Surface Scanner. Available in: < http://www.hoskin.qc.ca/uploadpdf/Instrumentation/Taylor%20Hobson/hoskin_TSCAN150_44ad086f7458b.pdf> Accessed in 8th of July 2015.

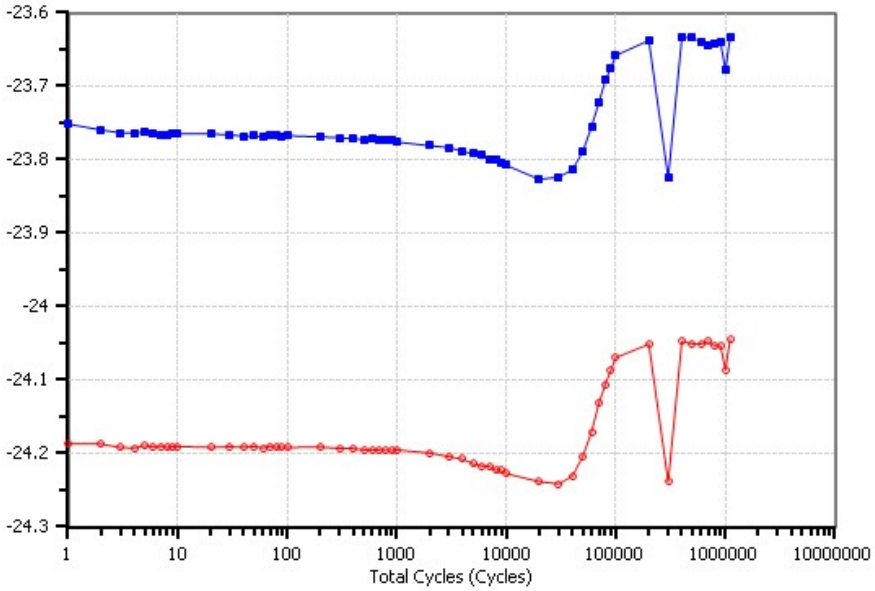
Light tool supply. Available in: < http://www.lighttoolsupply.com/catalog/Manufacturers/Mitutoyo/Mitutoyo-Surftest-SJ-210-Portable-Surface-Roughness-Tester > Accessed in 8th of July 2015.

Appendix.

1. Specimen M5T1(B).

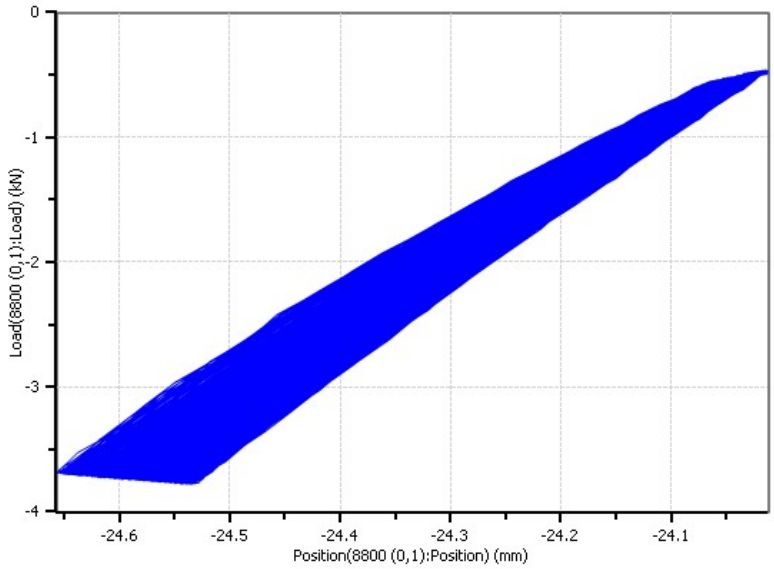


Load-displacement curve at the final phase of the fatigue test of the bristle blasted specimen tested under 60% of load level.

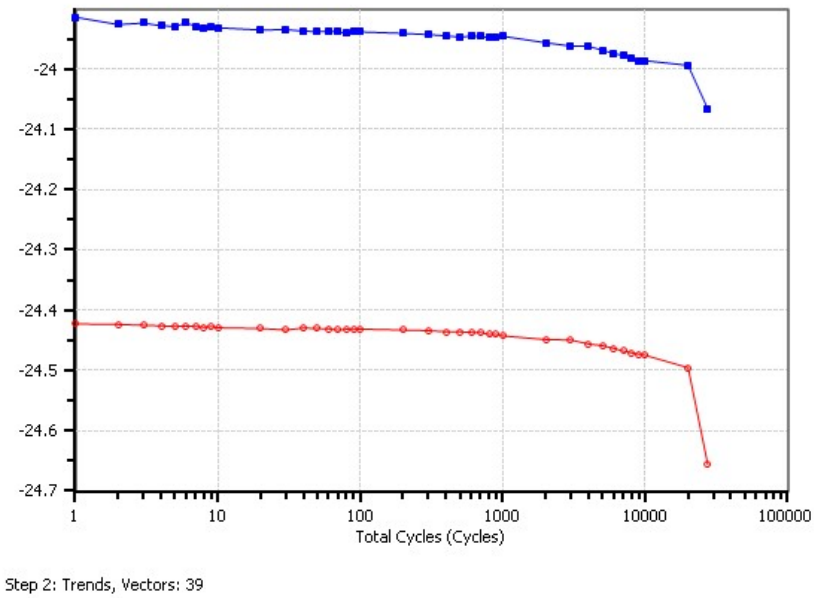


Displacement-Total cycles curve registered the fatigue life of 27,521 cycles of the specimen M6T1(C).

2. Specimen M6T1(C).

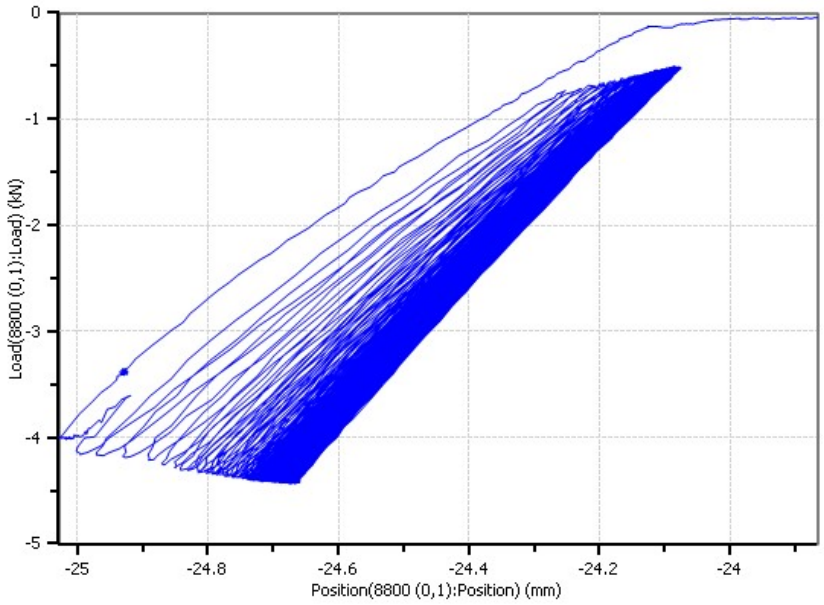


Load-displacement curve at the final phase of the fatigue test of the sand blasted specimen tested under 50% of load level.

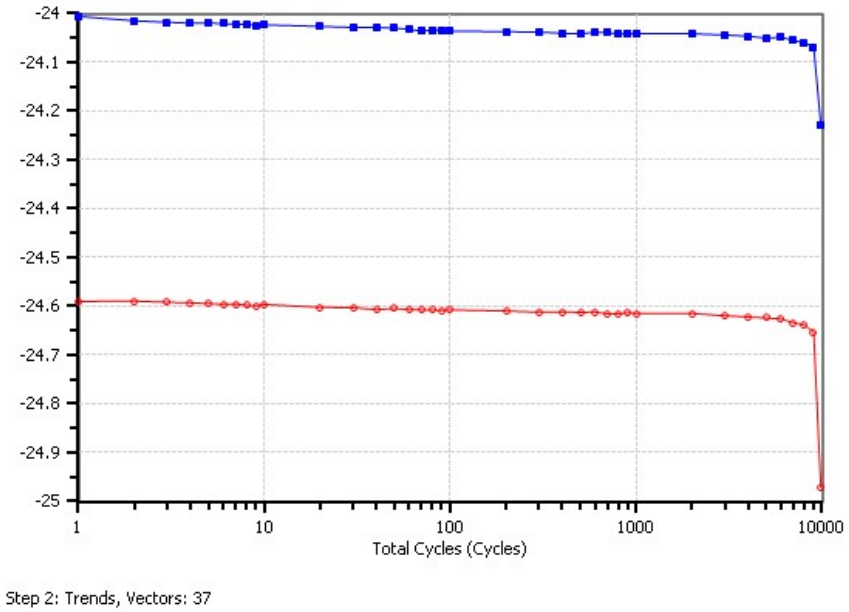


Displacement-Total cycles curve registered the fatigue life of 1,100,092 cycles of the specimen M5T1(B).

3. Specimen M7T3(C).

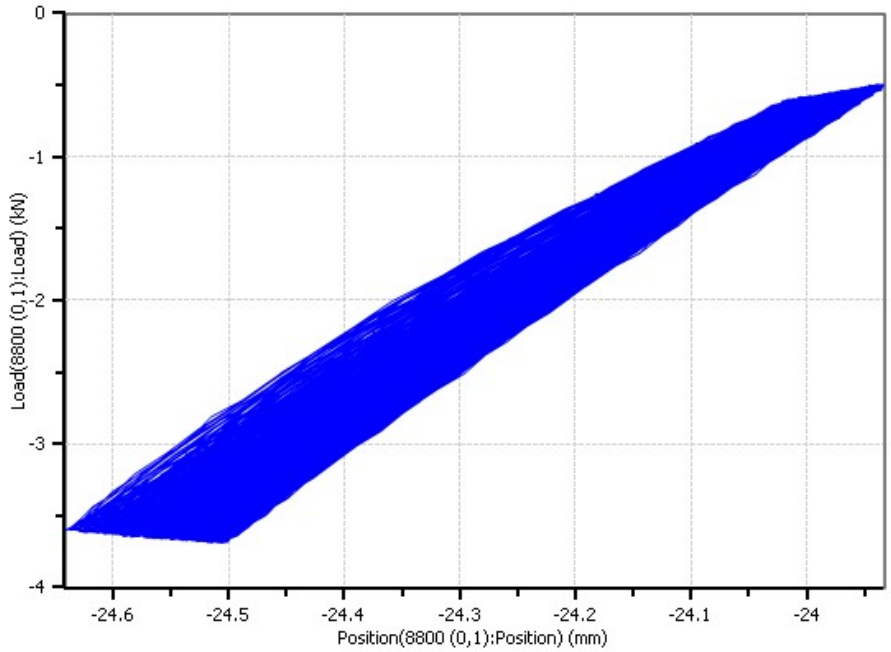


Load-displacement curve at the final phase of the fatigue test of the bristle blasted specimen tested under 70% of load level.

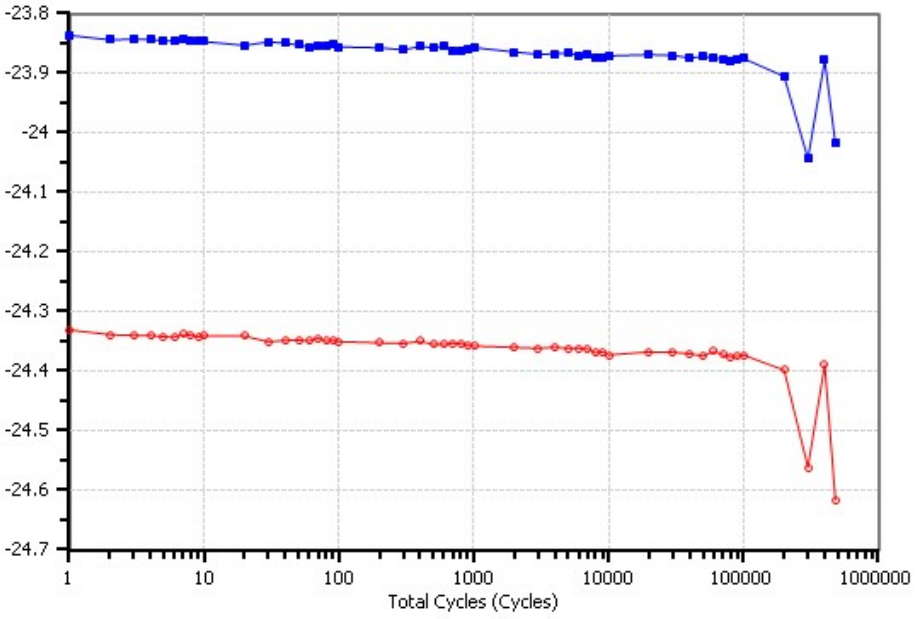


Displacement-Total cycles curve registered the fatigue life of 9,826 cycles of the specimen M7T3(C).

4. Specimen M6T3(A).

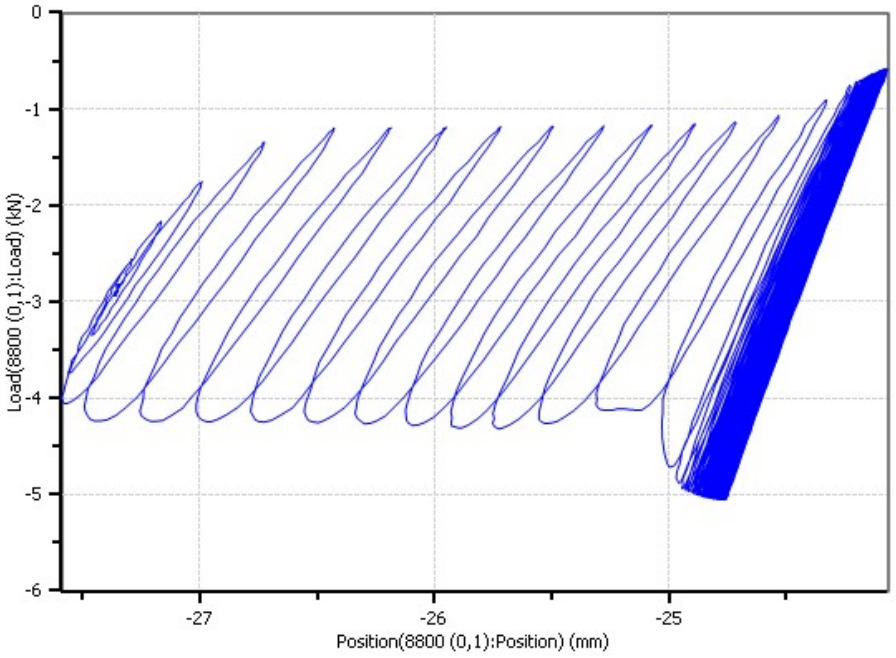


Load-displacement curve at the final phase of the fatigue test of the grit blasted specimen tested under 60% of load level.

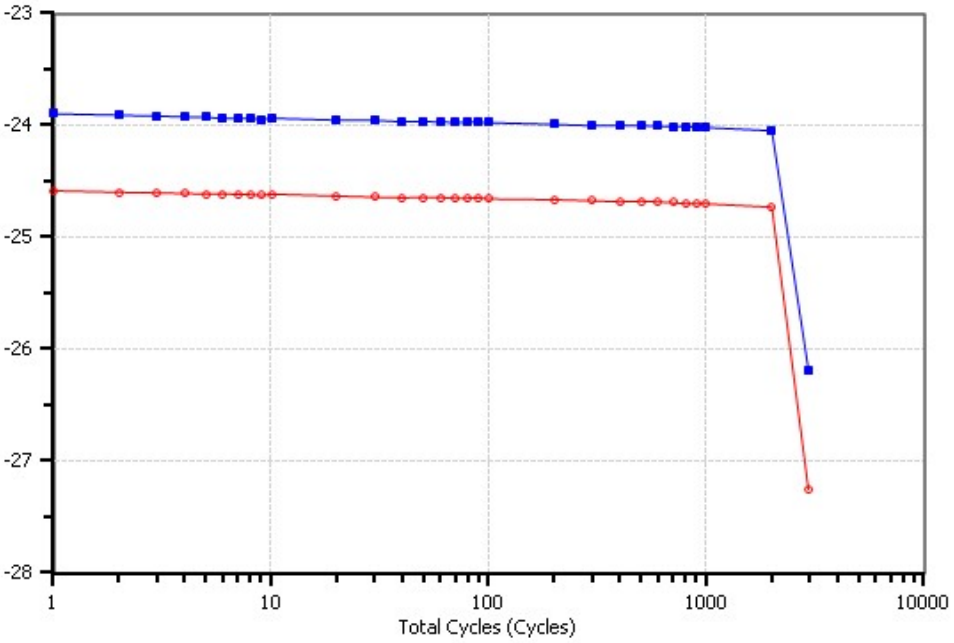


Displacement-Total cycles curve registered the fatigue life of 479,368 cycles of the specimen M6T3(A).

5. Specimen M8T3(A).



Load-displacement curve at the final phase of the fatigue test of the grit blasted specimen tested under 80% of load level.



Displacement-Total cycles curve registered the fatigue life of 2,942 cycles of the specimen M8T3(A).

Presentations of the work.

Congress presentations:

Poster:

Silvio de Barros, Paulo. P. Kenedi, Luis. F.G. de Souza, Svetlana N.M. Ferreira, A.J. Bernardino. *Influence of surface mechanical treatment on fatigue life of adhesively bonded joints under mode II loading.* XIV Brazilian MRS Meeting in Rio de Janeiro, 2015.

S. M. Ferreira, A.J. Bernardino, S. De Barros, P. P. Kenedi, *Influência da Rugosidade Superficial na Resistência à Fadiga de Juntas Metálicas Coladas,* Conferência Luso-Brasileira de Adesão e Adesivos, CLBA 2016.

Complete work:

Silvio de Barros, Paulo P. Kenedi, Luis F.G. de Souza, Svetlana N.M. Ferreira, A.J. Bernardino. *Influence of surface treatment on the fatigue life of bonded joints.* 3rd International Conference on Structural Adhesive Bonding AB2015, 2015.

Silvio de Barros, Paulo P. Kenedi, Luis F.G. de Souza, Svetlana N.M. Ferreira, A.J. Bernardino. *Influence of surface treatment on the fatigue life of bonded joints.* COBEM – 23th Brazilian Congress of Mechanical Engineering. Rio de Janeiro: ABCM, 2015.

Article:

Silvio de Barros, Paulo. P. Kenedi, Luis. F.G. de Souza, S. Budhe, Svetlana N.M. Ferreira, A.J. Bernardino. *Influence of surface mechanical treatment on fatigue life of adhesively bonded joints under mode II loading.* The Journal of Adhesion. DOI:10.1080/00218464.2015.1122531